Consequences of Gill Remodeling on Na^+ Transport in Goldfish, *Carassius auratus*

By

Julia Bradshaw

Thesis submitted to the
School of Graduate Studies and Research
University of Ottawa
In partial fulfillment of the requirements for the
M.Sc. degree in the
Ottawa-Carleton Institute of Biology

Thèse soumise à
L' École des etudes supérieurs et de la recherche
Université d'Ottawa
En vue de l'obtention du matrisse ès sciences à
L'Institut de biologie d'Ottawa-Carleton

ABSTRACT

Goldfish undergo an adaptive morphological change in their gills involving the reversible growth and loss of a mass of cells (interlamellar cell mass, ILCM) in between the lamellae depending on oxygen demand, which can be altered by the environment or metabolic demands of the individual. The ILCM contributes to decreased passive Na^+ efflux across the gill. Active uptake is maintained by the re-distribution of the ionocytes expressing Na^+-uptake relevant genes (NHEs and H^+-ATPase) to the outer edge of the ILCM where they can establish contact with the external environment and/or lamellar epithelium. This adaptation is thought to be partly responsible for the extreme anoxia tolerance demonstrated by goldfish, which they experience on a seasonal basis living in a pond environment. Hypoxia and hypercapnia are frequently encountered in such freshwater environments and as such, the effect of the ILCM on the capacity for acid-base regulation was evaluated. Differences in the time course of acid excretion to the environment without effect on systemic pH regulation were likely the result of the ILCM.

RÉSUMÉ

Les branchies des cyprins dorés (*Carassius auratus*) subissent un changement adaptatif impliquant la croissance ou la perte de la masse de cellules inter-lamellaire (MCIL) qui est dépendant sur leur demande d'oxygène, qui peut-être modifier par l'environnement ou les demandes métaboliques de l'individu. J'ai démontré que la MICL contribue à la réduction de la perte passive de Na^+ au travers de la branchie. L'absorption active est maintenue par le repositionnement des ionocytes, qui expriment les gènes pertinents à l'absorption du Na^+ (NHEs, H^+-ATPase), à la périphérie extérieure de la MICL, d'où ils sont en contact avec le milieu extérieur et/ou l'épithélium lamellaire. Cette adaptation est pensée d'être partiellement responsable pour l'extrême tolérance à l'hypoxie démontrée par les cyprins-dorés.

L'hypercapnie peut se produire dans des environnements tels que l'eau douce donc l'effet de la MICL sur la régulation acido-basique a été évalué. La capacité de réguler le pH sanguin n'a pas été modifié, cependant il y avait des différences significatives dans le mécanisme de compensation du pH utilisé et le décours temporel des échanges acido-basiques avec l'environnement qui reflétaient possiblement la présence ou l'absence de la MICL.

ACKNOWLEDGEMENTS

It is a pleasure to thank everyone that made this thesis possible. Firstly, I am indebted to my supervisor, Steve Perry, for giving me this opportunity and for his guidance along the way. His advice and humor made my experience meaningful.

My colleagues in the lab made sure that research was fun and engaging! Thanks to Villie for her help and entertainment during late night samples. I would like to say a big thanks to Yusuke for his ongoing help and advice and chats about science and Japanese culture. Thank you to Shelby for planning all the lab activities and for always teaching me something new. I would like to thank all the Biograds and the BGSA for making my experience here worthwhile.

I would also like to thank my advisory committee members, especially Pat Walsh and Katie Gilmour for their extremely thoughtful and detailed comments and constructive criticisms.

I greatly appreciate and would like to thank all of the support and technical staff in the Library, Aquatic Services, Science Stores and the Biology Department at the University of Ottawa for all their hard work and dedication.

I am grateful for my loving parents, Leonard and Claire Bradshaw, who have supported me, encouraged me and always pushed me to strive for more. Thank you especially for advice and sitting through endless practice presentations.

Last, but certainly not least, I would like to thank my fiancée, Glenn, for his continuous love and support. Thank you for always being a careful and patient ear. A special thanks goes out to Glenn for filling in part time as the lab social coordinator.

TABLE OF CONTENTS

LIST OF FIGURES

Chapter 3

Figure 4.2

Effect of hypercapnia exposure (P_wCO_2 = 10 mmHg) (A) titratable alkalinity ($J_{net}TA$), (B) ammonia $J_{net}Amm$ and (C) net proton equivalent fluxes ($J_{net}H^+$).

Figure 4.3

The effect of environmental hypercapnia exposure on $J_{in}Na^+$ in fish acclimated to 25°C (filled bars) and 7°C (unfilled bars).

Figure 4.4

The effect of CO2 exposure on relative mRNA expression of NHE3, NHE2 and H^+-ATPase in goldfish acclimated to 7°C (A) and 25°C (B).

LIST OF TABLES

Chapter 2

Chapter 3

Chapter 4

LIST OF ABBREVIATIONS

ANOVA analysis of variance

CO_2 carbon dioxide

DEPC diethylpyrocarbonate

EIPA N-ethyl-N-isopropyl amiloride

ENaC epithelial sodium channel

EtOH ethanol

FW freshwater

h hour

H^+-ATPase proton adenosine triphosphatase

Hb hemoglobin

HR cell H^+ pump rich cell

ILCM interlamellar cell mass

IPW ion poor water

$J_{in}Na^+$ Na^+ influx

J_{net}AMM

$J_{net}Na^+$ net Na^+ flux

J_{net}TA net titratable alkalinity

$J_{out}Na^+$ Na^+ efflux

LiCl lithium chloride

min minute(s)

MRC mitochondrion-rich cell

MO_2 oxygen consumption

MO_{2MAX} maximum rate of oxygen consumption

Na+/K+-ATPase sodium-potassium adenosine triphosphatase

NaR sodium pump (Na^+/K^+-ATPase) rich cell

NBC sodium-bicarbonate co-transporter

NCC Na+/Cl- co-transporter

NH_3 ammonia

NHE Na^+/H^+ exchanger

O_2 oxygen

P_aO_2 partial pressure of oxygen in arterial blood

P_aCO_2 partial pressure of carbon dioxide in arterial blood

PEG polyethylene glycol

PFA paraformaldehyde

pH_a arterial pH

PNA peanut lectin agglutinin

PVC pavement cell

P_wCO_2 partial pressure of carbon dioxide in water

Rh Rhesus

RTase reverse transcriptase

s second(s)

SEM standard error of the mean

SW seawater

TA titratable alkalinity

TJ tight junctions

UFR urine filtration rate

CHAPTER 1.

General Introduction

1.1 The fish gill: Considerations for a multifunctional organ

The fish gill is the organ responsible for gas exchange, acid-base and ionic regulation, and nitrogenous waste excretion. As such it acts as the interface between the internal and external environments. For the gill to function optimally in all its capacities, there is a requirement for both exchange *and* barrier functions. On the one hand, the capacity to achieve high metabolic rates requires efficient exchange of gases (oxygen (O_2) and carbon dioxide (CO_2)) across the gill, which in turn requires a large diffusing capacity. Conversely, to maintain ion homeostasis, the free movement of ions, small solutes and H_2O should be restricted, which would be best achieved by a gill possessing a low diffusing capacity.

A large volume of water is pumped continuously across the surface of the gills where O_2 diffuses across the lamellar epithelium into the blood. The net direction of diffusion of a given substance is determined by the prevailing concentration gradient (or partial pressure gradient in the case of a gas) and is governed by Fick's law of diffusion. Fick's law of diffusion tells us that the rate of molecular diffusion is directly proportional to the functional surface area and inversely proportional to the thickness of the barrier. Therefore, increasing the surface area and/or decreasing the thickness of the gill, enhances the diffusing capacity of the gill, allowing for a greater maximal rate of O_2 consumption (MO_{2MAX}) and a higher aerobic capacity (DeJagger and Dekker, 1975; Hughes, 1966) while presumably also contributing to greater rates of diffusion of salts and water. In addition to prevailing gradients, diffusive processes are also influenced by the permeability of the gill and in the case of ions, the electrical gradient across the gill. All of these physical parameters may be subject to change either as a consequence of

environmental perturbations or as a result of metabolic or endocrine changes within the fish.

Fish inhabiting a hypotonic, freshwater (FW) environment are subject to the continual loss of ions and absorption of water across the gills. For this reason, FW fish do not drink (or drink little), produce copious amounts of dilute urine and must balance their ion loss by actively taking up ions from the water across the gill epithelium. Although a gill epithelium with a large surface area will exhibit an increased capacity for O_2 transfer and thus enhance oxygen consumption (MO_2) and aerobic capacity, diffusive ion loss and water gain are inevitable and the energy expended in replenishing ions and producing urine places limitations on the maximum gill surface area (Randall et al., 1972). Estimates of the energetic cost of osmoregulation reported in the literature vary dramatically from 12% to 68% of overall metabolic rate (see Boeuf and Payan, 2001 for review). This trade-off is known as the *osmorespiratory compromise* (Randall et al., 1972; Nilsson and Sundin, 1986).

To accommodate this compromise of gill functions, fish (at least rainbow trout) at rest perfuse only a portion of the total gill with blood (Booth, 1978), using shunts to divert blood to the non-respiratory circulation of the filament (Farrell, 1980). While the gill surface area-to-body mass ratio is more-or-less a defined characteristic of a given group of fishes, the "functional" gill surface area and structural characteristics are dynamic, responding to environmental and internal stimuli. Before diving into the dynamic nature of gill morphology, a brief description of both the gross and cellular morphology and ion transport pathways of the gill is needed.

1.2 The gill epithelium: Structure and function

Gill structure has been studied extensively for over 50 years resulting in a vast accumulation of scientific data on morphology and ultrastructure from a variety of fish species (e.g. Hughes and Morgan, 1973; Perry, 1997; Wilson and Laurent, 2002). The gill epithelium is composed of at least four differentiated cell types; pavement cells, mucous cells, neuroepithelial cells and mitochondrion-rich cells. The cell types of primary interest to this thesis are the pavement cells (PVCs) and mitochondrion-rich cells (MRCs). Pavement cells are by far the most numerous in the gill epithelium and form the basis of the epithelial structure, on top of the basal lamina. While originally thought to play only a minor role in ion transport (Laurent and Perry, 1990) and typically described as containing few mitochondria, PVC sub-types were discovered to contain sub-apical vesicles containing H^+-ATPase (Laurent et al., 1994) and found to have substantial mitochondria compared to the standard PVC (Goss et al., 1992b). Their role in ion regulation and acid-excretion was subsequently investigated (Laurent et al., 1994; Sullivan et al., 1995). While sheer numbers of PVCs may augment their overall contribution to whole-animal osmoregulation and acid-base homeostasis (Perry, 1997), the principle cell-type responsible for ion regulation is the mitochondrion-rich cell (MRC). MRCs were originally referred to as chloride cells in marine species because of their role in Cl^- excretion. MRCs in FW fishes were also originally referred to as chloride cells because of their role in ion regulation. However, relatively recently, a more appropriate nomenclature, given the differences in both structure and function between the SW and FW types, was adopted and these cells are generally referred to as mitochondrion-rich cells or ionocytes (see Perry, 1997 for review). These cells possess

numerous mitochondria (to generate energy needed for active ion transport), an extensive tubular system (to facilitate transcellular movement of substances from apical to basolateral membranes), an extensive basolateral membrane and a complex apical surface with microplicae ridges (creating a large surface area). The ultrastrucutre of the apical surface of MRCs amongst species can be highly variable with differing densities and organization of microplicae; some species with a convex apical surface, raised above neighbouring PVCs and some with a concave apical crypt (a characteristic typical of the marine teleost chloride cell) (Perry et al., 1992). These differences in ultrastructure are thought to reflect adaptive changes to particular environmental conditions (Perry et al., 1992). MRCs comprise multiple subtypes that are thought to play different ionoregulatory roles. Elaborating the role of MRCs in ion transport is further complicated by different classification schemes used in the literature depending on the fish species in which they were characterized.

Rainbow trout (*Oncorhynchus mykiss*) MRCs are classified by the binding of peanut lectin agglutinin (PNA), a polysaccharide-binding protein found on the plasma membranes of specific cell types. PNA was originally found to bind specifically to the β-intercalated cells (base secreting cells) of the rabbit kidney (LeHir et al, 1982) and subsequently was also found to bind to a sub-type of trout gill MRCs (Goss et al., 2001) that are thought to be analogous to the ß-intercalated cells. The PNA^+ cells are thought to possess apical Cl^-/HCO_3^- exchangers and are the base-secreting cells. Cells that do not bind PNA, PNA^- MRCs, are believed to be acid-secreting cells (Galvez et al., 2001), similar to the α-intercalated cell of the mammalian kidney, which possess apical H^+-ATPase and Na^+/H^+ exchangers (NHEs). The differential activation of these MRC

subtypes comprises the rainbow trout model for ionic and acid-base regulation (see Gilmour and Perry, 2009).

The zebrafish (*Danio rerio*) model (Hwang and Perry, 2010) consists of three characterized MRC cell types: H^+ATPase-rich (HR) cell, Na^+-Cl^- co-transporter (NCC) cell and Na^+ pump (NaR) which are responsible for Na^+ uptake/acid excretion and ammonia excretion, Cl^- uptake and Ca^{2+} uptake, respectively.

The original MRC model for the euryhaline Mozambique tilapia (*Oreochromis mossambicus*) descriptively referred to three different MRC types as "wavy-convex", "deep hole" and "shallow basin" (Lee et al., 1996a). More recently, a model was proposed in which four mitochondrion-rich cell types are present under various conditions; these are referred to as Type I - Type IV MRCs, each possessing a unique physiological role (Hiroi et al., 2005). Presence, abundance and protein expression of these cell types are affected by FW to SW transfers (and *vice versa*) (Lee et al, 2000, Hiroi et al., 2005). Type II MRCs are considered the FW type and are typically smaller in size and apical opening diameter, while Type IV MRCs are found in SW acclimated fish and possess a deep apical crypt, often associated with other MRCs sharing the same opening and accessory cells (Hiroi et al., 2005). Expression of ion transport proteins in type II and type IV cells is consistent with ion uptake and ion secretory roles required for proper ion balance in FW and SW, respectively (Hiroi et al., 2005). Type I and III MRCs are MRC precursors – Type I is considered an immature MRC, while Type III cells are Type IV precursors, whose role is to act as a buffer for the change in dominant cell types that occurs during the FW to SW transition. Exposure to SW directs these cells to swiftly express an apical Cl^- channel to become Type IV SW MRCs (Hiroi et al., 2005).

The chloride cells in the goldfish (*Carassius auratus*) and crucian carp (*Carassius carassius*) gills have not been described or annotated in such detail. However, Kikuchi (1977) described goldfish mitochondrion-rich cells, as viewed with electron microscopy, in a typical MRC fashion – with numerous mitochondria, numerous apically oriented electron dense vesicles and somewhat oddly, an apical crypt and multicellular complexes more reminiscent of marine species. Two different MRCs were identified on the epithelium on the basis of their morphological characteristics – type A MRCs were larger with a very shallow and can be almost convex but wide apical opening and type B MRCs were smaller with a narrow but deep apical opening or pit (Lee et al., 1996b). The relative abundance of the A and B type MRCs found on the goldfish filaments was found to be responsive to external salinity changes ranging from FW to 5% SW (Lee et al., 1996b).

1.3 Ion transport pathways in the gill

Biological membranes are selectively permeable and as previously mentioned, certain cell types are therefore responsible for different ion uptake/regulation functions. This selectivity is determined from the differential expression of types and numbers of ion transporters and channels that are transcribed, translated, shuttled to or from the membrane, activated or deactivated – and allows regulation of these channels at many different levels of their production/activation. Ion movement across the gill epithelium can occur via one of two pathways; a *transcellular* or a *paracellular* route (Sardet et al., 1979; Isaia, 1982). The transcellular pathway involves passage through cell membranes of small permeable solutes and gases, regulated by the law of diffusion. Less permeable

solutes, charged particles or large substances (e.g. carbohydrates) cannot diffuse readily through the phospholipid bilayer and must move across the membrane with the help of transporters, channels or pumps. Through interactions with specific amino acids within the channels, substances passing through are discriminated based on charge or size, where some channels can be more promiscuous or selective than others. A significant portion of branchial Na^+ loss is thought to occur through the *paracellular* pathway (see Zadunaisky, 1984). Paracellular transport occurs at the junction between two cells. The movement of solutes through this pathway is regulated by tight junction (TJ) protein complexes that consist of occludin and claudin transmembrane proteins (for review see Cereijido and Anderson, 2001). The number, type and depth of the TJs proteins control the 'leakiness' of the gill. In seawater teleosts, the TJs between PVC-PVC and MRC-PVC are deep multi-strand complexes forming a 'tight' paracellular seal (Sardet et al., 1979), while the junctions between MRCs and between MRCs and accessory cells are shallow, single strand junctions that form a leakier epithelial seal (for review see Laurent, 1984). While originally thought to be non-discriminatory, recent studies have found that specific occludins and claudins can form specialized paracellular "channels" with size and charge selectivity of that similar to ion channels in the membrane (Colegio et al., 2002). Goldfish occludin immunostaining was found to be prominent in the gill, intermittently lining the cells within the lamellae and filament and was also widespread between cells in the interlamellar region (Chasiotis and Kelly, 2008). Further supporting its regulatory role in gill permeability, occludin expression in goldfish was increased upon exposure to ion-poor water (IPW) (Chasiotis et al., 2009) and changes in

transcription were elicited by cortisol, a mineralcorticoid and stress hormone in rainbow trout (Chasiotis et al., 2010).

1.4 Na^+ transport mechanisms

The mechanism(s) of Na^+ uptake in FW fishes has long been debated (for reviews see Marshall, 2002; Hwang and Lee, 2007; Parks et al., 2008), yet still remains poorly understood. Krogh (1938) first proposed that Na^+ is taken up in exchange for NH_4^+, an idea which was indirectly corroborated by Maetz and Garcia-Romeu (1964) who also proposed that either NH_4^+ or H^+ must be exchanged with Na^+. Shortly thereafter, with the use of transport-blocking drugs and *in vitro* perfused gill preparations, it was demonstrated that $Na^+/H^+(NH_4^+)$ exchange occurs on the apical membrane (Payan, 1978), a role for carbonic anhydrase in generating counter-ions for Na^+/H^+ and Cl^-/HCO_3^- exchange was established (Maetz and Garcia-Romeu, 1964; Kertstetter et al., 1970), and the requirement of basolateral Na^+/K^+-ATPase as the driving force maintaining low intracellular [Na^+] was demonstrated (Payan, 1978) . $Na^+/H^+(NH_4^+)$ exchange was the established Na^+ uptake mechanism in marine teleosts and remained uncontested in FW fish until Avella and Bornancin (1989), realizing the unfavorable thermodynamics of such a system in FW (for review see Parks et al., 2008), proposed a new model of Na^+ uptake; electrogenic proton transport coupled electrically to Na^+ influx through a channel (Avella and Bornancin, 1989). Both theories are consistent with the first order saturation kinetics and competitive inhibition by counter-ions in the medium shown by Na^+ uptake in FW animals (Maetz and Garcia-Romeu, 1964; Avella and Bornancin, 1989; Parks et al., 2008). A review of the literature reveals support for both hypotheses in the form of

immunocytochemical localization of both H^+-ATPase (Laurent et al., 1994; Lin et al., 1994; Sullivan et al., 1995) and NHEs (Ivanis et al., 2008) to the apical membrane of MRCs or PVCs; diminished Na^+ uptake rates in the presence of bafilomycin (H^+ATPase blocker) (Fenwick et al., 1999), amiloride (inhibits ENaC at low concentration and NHEs at high concentrations) and 5-N-ethyl-N-isopropyl amiloride (EIPA) (NHE-specific blocker) (Esaki et al., 2006); decreased H^+-ATPase expression in the presence of high external [Na^+] (Lin and Randall, 1993); increase of NHE-3 mRNA expression in low Na^+ FW (Yan et al., 2007); significantly decreased rates of Na^+ uptake in adult zebrafish exposed to bafilomycin but not amiloride or EIPA at concentrations that have been shown to inhibit Na^+ uptake in other species (Boisen et al., 2003), amongst many other demonstrations that support either hypothesis (for reviews see, Perry and Gilmour 2006; Evans, 2008; Hwang, 2009). Further, Na^+ uptake was significantly inhibited in goldfish exposed to four different NHE blockers (5-N, N-dimethyl amiloride (DMA), 5-N-methyl-N-isopropyl amiloride (MIA), EIPA and 5-N, N-hexamethylene amiloride (HMA)) and phenamil, an ENaC blocker, suggesting a prominent role by NHEs and/or ENaC in Na^+ uptake in this species (Preest et al., 2005). It is now widely held that Na^+ uptake is likely the function of a cooperative action of both NHEs and H^+-ATPases (Hwang, 2009), and both proteins have been co-localized to the HR cell in zebrafish (Yan et al., 2007).

Ammonia is a toxic end product of protein catabolism that is excreted across the gills and to a lesser degree by the kidney (for review see Randall and Wright, 1987). The clearance of ammonia in exchange for Na^+ (Maetz and Garcia-Romeu, 1964) was originally thought to occur in the ionized form, because of the high equilibrium constant, pK = 9.25) or alternatively as a gas (NH_3), diffusing directly through the epithelium.

However, the relatively recent discovery of rhesus glycoproteins (Rh) as ammonia (NH_3) channels in puffer fish (Nakada et al., 2007b), zebrafish adults (Nakada et al., 2007a), zebrafish larvae (Braun et al., 2009) and rainbow trout (Nawata et al., 2007) has helped develop a novel theory involving a $Na^+/NH_4^+(NH_3)$ metabolon model, in which ammonia, excreted as a gas through Rh proteins (down a partial pressure gradient from blood-to-water), acts as a sink for protons, via diffusion trapping, and creates a favorable gradient for either an NHE or H^+-ATPase Na^+ uptake mechanism, or both (see Wright and Wood, 2009, for review).

1.5 Acid-base regulation

Unlike most mammals, which can quickly regulate blood pH by altering ventilation to modify CO_2 excretion, fish possess little capacity for respiratory compensation of acid-base disturbances as a consequence of the already high ventilatory requirements associated with aquatic respiration. Acid-base disturbances in fish are remedied metabolically primarily through branchial extrusion of H^+ leading to accumulation of HCO_3^- in the plasma (for review see Goss et al., 1992b; Evans et al., 2005; Gilmour and Perry, 2009). Regulation of pH occurs via differential adjustments in the rates of Na^+ and Cl^- fluxes; an increase in Na^+ influx increases blood pH owing to the associated outward movement of H^+, while a decrease in Cl^- influx also raises pH because HCO_3^- ions are retained. Rainbow trout rely primarily on a reduction of Cl^-/HCO_3^- exchange with the environment to regulate blood pH during respiratory acidosis (Hyde and Perry, 1989), whereas the eel (*Anguilla anguilla*), lacking significant apical Cl^-/HCO_3^- exchange mechanisms, relies solely on increasing Na^+/H^+ exchange (Sherratt et al., 1964) and the brown bullhead (*Ictalurus nebulosus*) adjusts the fluxes of both ion-

exchange systems (Goss et al., 1992a). The whole-animal response to a respiratory acidosis has been evaluated in the common carp, a close relative of the goldfish, where carp were found to attribute 75% of their pH compensation to Cl^-/HCO_3^- exchange (Claiborne and Heisler, 1986).

1.6 Plasticity of the gill

Gill structure is plastic and responsive to both internal (hormones and systemic blood variables) and environmental stimuli. Environmental factors relevant to this thesis that drive changes in gill structure are dissolved O_2 content, ion concentration and pH of the ambient water. The generalized response to decreased dissolved O_2 content in most fish species is a decrease in heart rate (hypoxic bradycardia), increased blood pressure and hyperventilation. Hypoxic bradycardia (if accompanied by a lowering of cardiac output) increases the transit time of the blood in the gill to potentially provide more time for O_2 diffusion and Hb-saturation. Increasing the blood pressure forces distal lamellar blood channels to open and increases the effective gill surface area utilized for gas exchange, while hyperventilation brings more oxygenated water over the gills. These physiological responses effectively increase the surface area of the gill available for gas exchange (functional surface area) and act to enhance O_2 uptake. Rainbow trout exposed to softwater (Goss et al, 1993; Greco et al., 1995), elevated plasma cortisol (Bindon et al., 1994), lowered NaCl (Perry and Laurent, 1989) or heavy metals (Evans et al., 1988), experience an increase in the MRC fractional area on the lamellae. This increase in either size and/or number of chloride cells results in an increase in the blood-to-water diffusion distance (Greco et al., 1995; Greco et al., 1996). The increased thickness of the diffusion

barrier was postulated to decrease the permeability of the gill (Greco et al., 1996) as was demonstrated in rainbow trout exposed to softwater in a previous study (McDonald and Rogano, 1986). The increase in lamellar thickness resulted in an impairment of O_2 transfer and imposed a diffusion limitation on CO_2 excretion in the rainbow trout (see Perry, 1998). While the role of cortisol in gill permeability will not be investigated in this thesis, it is noteworthy that an injection of cortisol, a stress hormone, elicits the same effect as softwater on the CC morphology of the gill – cellular hypertrophy and proliferation (Laurent and Perry, 1990). It should also be noted that increases in plasma cortisiol associated with stress do not result in changes of gill morphology (Sloman et al 2000). Conversely, during periods of acidosis in bullhead and trout (e.g. from exposure to a low pH or hypercapnic environment), pavement cells physically cover neighboring chloride cells, reducing their functional surface area. A reduction in the exposed apical surfaces of chloride cells reduces the activity of Cl^-/HCO_3^- exchange and simultaneously increases the contribution of Na^+/H^+ exchangers located on pavement cell membranes (Goss et al., 1993).

The Amazonian Oscar, living in environments where it is exposed to frequent and severe hypoxia in ion-poor water (IPW), provides a dynamic example of the osmorespiratory compromise at the cellular level. When exposed to hypoxia, this fish tightens up the gill and decreases transcellular efflux of ions without hindering O_2 uptake (Wood et al., 2009). They are thought to increase the coverage of the gill by pavement cells, thereby covering the apical crypts of MRCs to effectively uncouple ion channels/transporters from the water (Wood et al., 2009). This gill restructuring is achieved on the scale of hours and is reversible on the same time scale as fish are

returned to normoxia (Wood et al., 2009). A more radical change to gill morphology referred to in this thesis as gill remodeling has been demonstrated in several cyprinids including the goldfish. The consequences of this potentially adaptive morphological change form the questions that this thesis will address.

1.7 Gill remodeling

Gill remodeling involves the growth/loss of a mass of cells called the interlamellar cell mass (ILCM) between adjacent lamellae under particular environmental conditions. Goldfish acclimated to 25°C exhibit a gill phenotype, typical of most fish, that is, without an ILCM. When acclimated to colder temperatures (<15°C), the ILCM is present (Sollid et al., 2005). Goldfish thus provide an excellent model to evaluate the "osmorespiratory compromise" balancing act. The presence of an ILCM decreases the surface of the gill exposed to the environment (Sollid et al., 2003; Mitrovic et al., 2009) and presumably increases the blood-to-water diffusion distance. Fish in colder temperatures, have lower metabolic rates and therefore a decreased demand for O_2. The goldfish, therefore, remodels the gills and shifts the balance of gill function to optimal osmoregulation, by imposing a physical barrier. When metabolic rate is increased (i.e. with warmer temperature acclimation), the ILCM is shed through a combination of apoptosis and decreased cell growth (Sollid et al., 2006) and lamellae are re-exposed to the environment. The so-called osmorespiratory balance is tipped the other way, enhancing the ability of the gill to transfer respiratory gases. Cold-acclimated fish exposed to a hypoxic environment will also shed the ILCM to increase the surface area

available for O_2 uptake (Sollid et al., 2003). While the exact mechanism and proximate stimulus for gill remodeling has not been determined (Sollid et al., 2006), the primary driving force appears to be the O_2 demand of the individual or the environmental O_2 availability.

Branchial Cl^- permeability, as measured by Cl^- flux across the gill under remodeling conditions, was found to be regulated independently of the cell mass (Mitrovic and Perry, 2009). PEG efflux, on the other hand, was decreased 2.5 fold by the presence of the cell mass at warm temperatures, suggesting a decrease in overall permeability of the gill and a re-distribution of MRCs (demonstrated through visualization of MRC markers of Na^+/K^+-ATPase and mitochondria) to the edge of the cell mass where they are presumed to be involved in ion uptake from the environment (Mitrovic and Perry, 2009). The effect of the cell mass on cation transport has not been evaluated.

1.8 Anoxia-tolerance of goldfish

Goldfish are extremely anoxia/hypoxia tolerant and are able to survive in ice-covered ponds with little to no oxygen for several months, conditions under which they must rely on anaerobic energy production (Lutz and Nilsson, 1997). It is thought that gill remodeling allows goldfish to conserve energy and maximize storage and growth of liver glycogen reserves, whereby the amount of stored liver glycogen determines the anoxic survival period in overwintering goldfish (Nilsson, 2007). During the months preceding pond ice-formation, cooler temperatures prompt the growth of the ILCM. The ILCM, presumably decreasing the energetic cost of osmoregulation, in conjunction with a further decrease in energy expenditure as metabolic rate falls in low temperatures allows

the goldfish to convert these energy savings to glycogen stores. The period preceding anoxia is likely to be characterized by progressive hypoxia and shedding of the cell mass will preserve the oxygen consumption at lower environmental PO_2 and delay the metabolic switch to anaerobiosis (Nilsson, 2007). Metabolic end products (i.e. lactic acid) accrued during the anoxic period are converted into acid-base neutral ethanol and excreted via the gills (Shoubridge and Hochachka, 1980). This adaptation is thought to occur seasonally in goldfish and may be widespread among cyprinids. Gill remodeling has also been observed in, indeed was originally documented in, crucian carp (Sollid et al., 2003, 2005), Qinghai carp (Matey et al., 2008), as well as the more distant, Mangrove killifish (Ong et al., 2007). On top of the drastic seasonal changes to temperature and oxygen content, a pond environment encourages thermal stratification and episodes of relative hypoxia or hypercapnia as a result of non-mixing or the diurnal sun exposure cycle (see Diaz, 2001).

1.9 Goals and hypotheses

The goal of this thesis is to investigate the consequences of the interlamellar cell mass for the ion transport and acid-base physiology of goldfish. Extensive work has been done to characterize the causes of gill remodeling (Sollid et al., 2003, 2005), the effect on MO_2 (Sollid et al., 2005) and the effect on Cl^- flux (Mitrovic et al., 2009) as well as to try to determine the benefits and costs of such a dramatic change in gill structure (Sollid and Nilsson, 2006). To my knowledge, no prior research has investigated the consequences of gill remodeling on branchial Na^+ transport or systemic acid-base regulation. This thesis is written as two manuscripts to be submitted for publication, which form the data

chapters (Chapters 2 and 3). A single Materials and Methods section addressing both data chapters is included to reduce repetition.

Hypotheses:

1. *The ILCM will reduce the passive diffusion of Na^+ ions by decreasing the branchial surface area and increasing the blood-to-water diffusion distance.*
2. *Given the re-distribution of MRCs in the ILCM, Na^+-transporting cells will be similarly re-distributed to the edge of the ILCM.*
3. *Recovery from an acid-base insult will not be impeded in fish with an ILCM [due to the re-positioning of MRCs to the edge of the branchial epithelium].*

Chapter 1 sets the context for this thesis and introduces key concepts and background information. Here I have laid out the rationale for investigating the consequences of the gill remodeling strategy in goldfish. Chapter 2, the first data chapter, evaluates Na^+ flux across the gill under various environmentally induced gill phenotypes (with respect to the presence or absence of an ILCM). Physiology, molecular biology and histology are combined to provide a more complete rendering of the consequences of the presence of an ILCM. Chapter 3 addresses Na^+ transport as a mechanism of acid-base regulation. An acid-base disturbance was introduced to thermally acclimated goldfish to evaluate the effect of the ILCM on Na^+ and other acid-base relevant ion transport (H^+, HCO_3^-). Chapter 4 concludes by tying together the effect of the ILCM on Na^+ and acid-base homeostasis in goldfish and discusses relevant future directions to more fully comprehend the nature of and physiological effects of the ILCM.

CHAPTER 2

MATERIALS AND METHODS

2.1 Animal Care and Experimental Conditions

Goldfish (*Carassius auratus)* were purchased from Aleong's International (Mississauga, Ontario, Canada) and housed at the University of Ottawa in fiberglass tanks supplied with flowing, aerated and dechloraminated City of Ottawa tap water ($[Na^+]$ = 0.7 mM, $[Ca^{2+}]$ = 0.2 mM, $[Cl^-]$ = 0.4 mM; pH 7.4-7.6). We were unable to take successive blood samples from fish < 100 g, therefore two different size classes of fish were used: 22.0 ± 0.6 (SEM) g (N = 80) for flux and titration experiments and150.6 ± 4.8 g (N = 12) for blood acid-base experiments. The fish were maintained under a 12h: 12h light: dark photoperiod and fed commercial pellets *ad libitum* on a daily basis. Fish were acquired at a holding temperature of 18°C and acclimated to their experimental temperatures (25°C or 7°C) by adjusting water temperature at the rate of 2°C per day. All fish were held at their experimental temperatures for at least 2 weeks prior to experimentation to ensure that gill remodeling was complete. All experiments using live animals were performed according to institutional guidelines in line with the Canadian Council on Animal Care (CCAC). Prior to experimentation, fish were transferred to individual opaque chambers (~500 ml) and allowed to acclimate to their environment for 24 h.

Fish were made hypoxic by supplying the holding chambers with water made hypoxic through gas-water column equilibration using a mixture of N_2 and air (GF-3/MP gas mixing flowmeter, Cameron Instrument Company) to achieve a final PO_2 of ~ 10 mmHg and maintained under these conditions for 7 days. In a recovery group, fish were returned to normoxia (PO_2 ~ 156 mmHg) for a 12 h "recovery" period prior to experimentation. Water PO_2 was measured using a polarographic oxygen electrode and

associated oxygen meter (OM200 Oxygen Meter, Cameron Instruments) (Cameron Instruments, Analytical Sensors). The O_2 electrode was calibrated with zero solution (2 g 100 mL^{-1} sodium sulfite) and air-saturated water.

Hypercapnia was achieved by bubbling a gas exchange equilibration column with 3% CO_2 in air to achieve a final P_wCO_2 of ~ 10 mmHg in water supplying the experimental chamber. For all experiments, fish were exposed to hypercapnia for 48 h. Water PCO_2 was monitored with a CO_2 microelectrode (Microelectrodes Inc., Bedford, NH, USA) connected to a blood gas meter (Model BGM200, Cameron Instruments), monitored by Biopac data acquisition logger ((UIM100A and MP100A-CE, Biopac Systems Canada, Montreal, QC, Canada) and Acknowledge software (Version 3.73, Biopac Systems Canada, Montreal, QC, Canada) running on a PC and calibrated with water equilibrated with 0.5% and 1% CO_2 (GF-3/MP gas mixing flowmeter, Cameron Instruments).

Hyperoxia was achieved by in the same manner as hypercapnia and hypoxia (see above), but using 100% O_2 to achieve a final water PO_2 of ~300 mmHg. Fish were exposed to hyperoxia for 10 minutes prior to ventilation rate measurements and 12 h prior to flux experiments.

2.2 Na^+ fluxes and plasma analysis

Na^+ influx ($J_{in}Na^+$) and net flux ($J_{net}Na^+$) were measured simultaneously while Na^+ efflux ($J_{out}Na^+$) was measured in a separate group of fish. Fish were weighed and placed into individual flux chambers (~500 mL) that were supplied with flowing water. For influx experiments, water flow to the chambers was halted and 1 μCi ^{22}Na in the

form of NaCl (SA of stock 830.19 mCi/mg; Perkin Elmer, Waltham, MA, USA) was added to the flux chamber. Chambers were aerated with room air (controls, normoxic groups), N_2/air mix (hypoxia) or O_2 (hyperoxia) during the experimental flux periods. Following a 15-min mixing period, 20 mL water samples were taken at 1 h intervals over a 4 h period for measurements of ^{22}Na and $[Na^+]$. The radioisotope activity was measured with a liquid scintillation counter (LS 6500 Multi-Purpose Scintillation Counter, Beckman Coulter, Brea, CA,USA) using a mixture of 15 mL of counting cocktail (BIOSAFE II, RPI corp., Mt. Prospect, Ill, USA) and 4 mL of water sample. Counts per minute (CPM) were converted to disintegrations per minute (DPM) using a quench correction value calculated by the counter with an external quench monitor using ^{137}Cs as a standard. Water $[Na^+]$ was measured with an atomic absorption spectrometer (AA260, Varian, California, USA) calibrated with certified Na^+ standards (SCP Science, Baie D'Urfé, QC, Canada). $J_{in}Na^+$ was calculated according to the formula:

$J_{in}Na^+ = [\Delta H_2O\ ^{22}Na\ (DPMh^{-1}) / H_2O\ ^{22}Na$ specific activity $(DPM\ \mu mol^{-1})] /$ fish mass (kg). Mean water ^{22}Na specific activity was determined from the measurements taken at 0 and 4 h. The decrease in ^{22}Na over the flux period was linear ($r^2 = 0.97 \pm 0.01$) and less than 10% ($9.1 \pm 1.3\%$) of the starting activity. Net flux was calculated from the following formula: $J_{net}Na^+ = [([Na^+]_i - [Na^+]_f)(\mu mol/L)$ X volume of H_2O (L)]/[fish mass (kg) X time (h)]. Owing to the potentially stressful nature of the efflux experiments, net flux values were only measured during influx experiments where no surgical procedures were involved. Backflux corrections were not applied because the internal specific activity (assuming 40 mmol kg^{-1} internal pool of Na^+) was not more than 5% of the external specific activity (Maetz, 1956).

For efflux experiments, 1 μCi ^{22}NaCl (Perkin Elmer, Waltham, Massachusetts, USA) (vol. 20 uL) was injected into the peritoneal cavity, after which fish were allowed to recover for 12 h. Fish were then anaesthetized (ethyl-4-amino-benzoate, 6.05 X 10^{-5} mol L^{-1}, Sigma Aldrich, St. Louis, Missouri) and the anal vent sutured to prevent contamination of the water by urinary Na^+ as outlined previously (Mitrovic et al., 2009; Mitrovic and Perry, 2009). Fish were allowed to recover from anaesthetic for 2 h prior to measurements. Flow to chambers was stopped, chambers were aerated as described above and water samples (20 mL) were taken every hour for 4 h. Samples were measured for ^{22}Na and [Na^+] as described previously. After terminal anaesthesia (ethyl-4-amino-benzoate, 6.05 X 10^{-3} mol L^{-1}) blood samples were collected via caudal puncture, separated by centrifugation at 5000 x g for 3 min and plasma was assessed for both ^{22}Na (15 mL counting cocktail + 4 mL H_2O + 100 μL plasma) and [Na^+] (1:10000 dilution in distilled H_2O). $J_{out}Na^+$ was calculated using the formula; $J_{out}Na^+$ = [Δwater ^{22}Na (DPM h^{-1})/ plasma ^{22}Na specific activity (DPM μmol^{-1})]/ fish mass (kg). The average rate of Na^+ appearance was calculated from the linear regression of activity over time throughout the 4 h flux period.

The Na^+ flux measurements taken from hypercapnia exposed fish were taken over 3 h intervals, following the methods of Perry et al., 1987.

2.3 Branchial ammonia and acid fluxes

A colorimetric ammonia assay employing the salicylate method (Verdouw et al., 1978) was used to measure ammonia concentrations of water samples at t = 0 and 3 h for each flux period. Water samples taken at the beginning and end of the flux periods were

titrated to an end-point of pH 4.0 with 0.02 M HCl. An automatic titrator was used (Model 836 Titrando, Metrohm, Switzerland) coupled with a combination pH electrode (Metrohm AG 9101) and values recorded as averages of duplicates. In brief, samples (5 mL) were stirred continuously and titrated rapidly to pH 4.5. After 15 min of aeration to remove additional CO_2, the sample was titrated to pH 4.0. The volume and concentration of titrant added to the initial and final water samples were used to calculate the titratable component of the net acid flux ($J_{NET}TA$) according to the method of McDonald and Wood (1981). This component reflects only one part of the excreted acid; the other component is attributed to ammonia excretion ($J_{NET}AMM$). Thus, total net acid excretion ($J_{net}H^+$) = $J_{net}TA + J_{net}Amm$ (with signs considered).

2.4 Blood acid-base analysis

Large goldfish were anesthetized in an oxygenated solution of benzocaine (6.05 X 10^{-5} mol L^{-1} ethyl-4-amino-benzoate) and transferred to a surgery table where the gills were irrigated for the duration of the surgery with oxygenated, diluted anesthetic. A cannula was inserted and secured in the caudal artery as described in Tzaneva et al. (2010). Fish were allowed >12h to recover in 3000 mL plastic containers supplied with aerated flowing water. The inflowing water was then made hypercapnic, as previously described, and 0.3 mL blood samples were withdrawn from the caudal artery at 0, 0.5, 3, 12 and 48 h of hypercapnia exposure. Whole blood was kept in a 1 mL plastic syringe sealed with parafilm and analyzed immediately. pH was measured statically using a temperature-controlled (to either 7°C or 25°C) electrode-chamber housing a reference electrode (E351, Analytical Sensors, Inc.) and pH electrode (PH-CM, Analytical Sensors,

Inc.) connected to a blood gas meter (Cameron Instruments). Blood was subsequently withdrawn and spun in a 1.5 mL centrifuge tube at 5000 x *g* for 3 min. Plasma was withdrawn into 50 µL gas-tight syringes (Hamilton, Reno, Nevada, USA) and analyzed for total CO_2 content with a carbon dioxide analyzer (Corning 965, Corning Ltd, Halstead, Essex, UK).

2.5 Hyperoxia and ventilation rates

Fish were fitted with an opercular cannula (PE 90, Clay Adams Dynac, BD Diagnostic Systems, New Jersey, USA) that was heat-flared on one end and secured in place with a silk ligature. A physiological pressure transducer (Statham Transducers, Model P23AC) and manometer system, continuous with the opercular cannula recorded changes in pressure resulting from movements of the opercular flap during each ventilatory cycle. The pressure transducer was calibrated against a column of water and data were recorded with a BIOPAC data logger acquisition system (UIM100A and MP100A-CE, Biopac Systems Canada, Montreal, QC, Canada) and Acknowledge software (Version 3.73, Biopac Systems Canada, Montreal, QC, Canada) running on a PC.

2.6 Gill Arch Cryosectioning

Gill arches were excised and rinsed in ice-cold phosphate-buffered saline. The first and second gill arches were removed and gill filaments were fixed in 4% paraformaldehyde (Sigma Aldrich) in phosphate-buffered saline overnight at 4°C. The gill samples were then cryoprotected for 24 h in a series of sucrose solutions (15%

overnight followed by 30%). Gills were embedded in optimal cutting temperature embedding media (Cryomatrix; Shandon, Pittsburgh, Pennsylvania, USA), frozen in liquid N_2, and stored at -80°C until sectioning. Gills were sectioned on a cryostat microtome (Leica CM3350, Leica Microsystems, Richmond Hill, Ontario, Canada) at -30°C using disposable microtome blades (MX35 Premier microtome blade, Thermoscientific, MA, USA). Sections were 10 μm thick and placed on Superfrost plus slides (Fisher Scientific). Slides were dried at room temperature for 1 h prior to freezing and storing at -20°C.

2.7 Cloning of partial-length cDNA

The first gill arch was homogenized using a mortar and pestle (Fisher Scientific) under liquid N_2. Total RNA was extracted from 10 mg ground gill tissue using TRIzol (Invitrogen, California, USA) RNA extraction solution. Total RNA was treated with DNase (Fermentas Life Sciences, Burlington, Ontario, Canada) for 12 min at room temperature and 2 μg RNA was reverse transcribed with RevertAID H Minus reverse transcriptase (Fermentas Life Sciences) and primed with random hexamers (Invitrogen), following the protocol of the manufacturer. Forward and reverse primers were developed for H^+-ATPase and NHE3 (Table 1) from expressed sequences tags published on NCBI located using the GOLDarrayALL.nt database (http://137.122.149.18/blast/). Degenerate primers for NHE2 were developed using known fish and tetrapod sequences from Towle et al. (1997) (3F) and Edwards et al. (2010) (NHE-R; Table 1). Polymerase chain reaction (PCR) products for H^+-ATPase, NHE3 and NHE2 were amplified, cloned and sequenced using standard protocols established in our laboratory (e.g. Perry et al., 2003).

A nucleotide BLAST of GenBank databases using the cloned H^+-ATPase, NHE3 and NHE2 sequences as queries revealed high sequence identity (>80%) with known zebrafish sequences. Clones were stored as glycerol stocks at -80°C.

2.8 RNA extraction and cDNA synthesis for real-time PCR

The first gill arch was homogenized with TRIzol (Invitrogen), as described in the previous section, the RNA so extracted was quantified spectrophotometrically with a NanoDrop analyzer (NanoDrop Technologies, Rockland, DE). RNA was treated with DNAse (Fermentas Life Sciences) by mixing 2 µg RNA (in 5 µL volume) with 1 µL DNAse and 1 µL DNAse buffer and incubating for 12 minutes at room temperature. The reaction was stopped by the addition of 1 µL EDTA (Invitrogen) and heating for 10 minutes at 65ºC. Following DNAse treatment, cDNA synthesis with RevertAID H Minus Reverse Transcriptase (Fermentas Life Sciences) was carried out according to the manufacturer's protocol. cDNA was purified using a PCR purification kit (Qiagen, Hilden, Germany). A negative control (no RTase) was prepared from a random RNA sample in which the RTase enzyme was not added. Real-time PCR was performed with an MX 3000 Multiplex Quantitative PCR System (Stratagene, Agilent Technologies, Santa Clara, USA) and Brilliant SYBR II QPCR master mix (Stratagene). The reaction mix was prepared according to manufacturer's protocol with the following modifications; reaction volume was 12.5 µL, primers were used at a final concentration of 50 nM and 2.5 µL of cDNA template was used. No RTase and no template negative control samples were run under the same conditions to check for genomic DNA contamination. Reactions were run using MXPro software version 4.0 (Stratagene) generalized SYBR

green PCR program with an annealing temperature of 58°C. Dissociation curves for the PCR products were constructed at the end of each run to ensure the presence of a single amplicon. All real-time PCR data were analyzed using the ΔΔCT method (Pfaffl, 2001). All genes are expressed relative to 18s ribosomal RNA reference gene expression and relative to a control gene.

Primers for real-time PCR (Table 2) were designed using web-based software (Primer3; http://frodo.wi.mit.edu/cgi-bin/primer3/primer3_www.cgi) based on goldfish partial cloned sequences for NHE3, NHE2 and H^+-ATPase. Standard curves were generated from serially diluted pooled cDNA to calculate PCR efficiencies (Table 2).

2.9 In situ hybridization

Plasmid DNA was isolated from bacterial clones containing the desired sequence (QIAprep Spin Miniprep Kit, Qiagen) and linearized by PCR with SP6 and T7 promoter primers (0.5 μL of plasmid DNA template was used and final primer concentration was 200 nmol L^{-1}; annealing temperature 46°C for 40 sec and extension at 72°C for 2 min over 35 cycles). Sense and anti-sense probes for H^+-ATPase (678 bp) and NHE3 (782 bp) were synthesized *in vitro* using SP6 and T7 RNA polymerases (New England BioLabs, Ipswich, Massachusetts, USA). A total of 2 μL of PCR-linearized template (using SP6 [5'-GAT TTA GGT GAC ACT ATA G-3'] and T7 [5'-TAA TAC GAC TCA CTA TAG GG-3'] primers; thermal cycling pattern consisted of 94º C for 3 min, followed by 35 cycles of 94º C for 40 s, 47º C for 40 s, 72º C for 2 min) was used in the reaction and incubated for 3 h at 37°C following the protocol of Smith et al., (2008). Probes were purified by lithium chloride (LiCl) precipitation overnight in 100% ethanol

(EtOH) and resuspended in 10 µL of diethylpyrocarbonate (DEPC) treated H_2O. Probe sizes were confirmed by gel electrophoresis and quantified by spectrometry (NanoDrop Technologies, Rockland, DE). Slides were defrosted for 1 h prior to hybridization overnight in a humidified chamber at 70°C. Probes were used in hybridization buffer (1x salt (10x composition: 2M NaCl, 90 mM Tris-HCl, 10 mM Tris base, 50mM NaH2PO4 H2O, 50 mM Na2HPO4, 0.5M EDTA), 50% ultrapure formamide (OmniPur deionized formamide, Fisher Scientific), 10% dextran sulphate (BIOSHOP Canada), 1mg/mL yeast tRNA (Invitrogen), 1x 50x Denhardt's (Invitrogen) in DEPC H_2O) at a final concentration of 1 nmol L^{-1}. Post-hybridization washes were 2 x 30 min in Solution A (50% formamide (BioShop Canada, Mississauga, Ontario), 1X SSC (20x SSC composition: 3M NaCl 0.3 M sodium citrate) in DEPC) at 70°C followed by 2 x 30 min washes in tris-buffered saline with 1% triton-X 100 (TBS-T) at room temperature. Slides were blocked for 1 h in 10% heat-inactivated goat serum in TBS-T at room temperature, followed by an overnight incubation in anti-dioxigenin-alkaline phosphatase conjugated antibody at 4°C. Slides were then washed 4 x 20 min in TBS-T at room temperature followed by 2 x 10 min washes in NTMT (100mM NaCl, 100 mM Tris HCl pH 9.5, 50 mM $MgCl_2$, 1% Triton-X 100 in H_2O) solution, followed by chromogenic staining using 5-Bromo-4-Chloro-3-Indolyphosphate p-Toluidine Salt and Nitro-Blue Tetrazolium Chloride tablet (Sigma Aldrich) dissolved in 10 mL NTMT until desired staining was achieved (6 - 14 h).

2.10 Statistical analysis

All statistical analyses were performed using SigmaStat software (Version 11.0, SPSS Inc., Chicago, IL, USA). In chapter 2, statistical significance of Na^+ flux and real-time PCR data was determined by student's t-test where $P < 0.05$. In chapter 3, statistical significance was determined by 2-way repeated measures analysis of variance (ANOVA), where $P < 0.005$. All data are presented as means ± 1 SEM.

Chapter 2 Tables and Figures

Table 2.1 Primers used in PCR for partial cloning and RNA probes synthesis for *in situ* hybridization

Target gene	Product Length (bp)	Sequence
NHE3	780	F-NHE3-GF: 5'-GCT GTT GAC CCT GTG GCT GT -3'
		R-NHE3-GF: 5'-GAC AGT GAA ATT CAC CAC AAT GA-3'
H^+ATPase	717	F-HATPase-GF: 5'-ATT GAA CGC ATC ATC ACC CC -3'
		HATPaseR1/2: 5'-AGC GAC TCC TCG GGT AGA TTC -3'
NHE2 (degenerate)	700	3F: 5'-AAY GAY GSN GTN CAN GTN GT -3'
		NHE-R: 5'-GNA GGC CAC CGT AGG C-3'
SP6/ T7 promoter	Variable	5' -GAT TTA GGT GAC ACT ATA G- 3'
		5'-TAA TAC GAC TCA CTA TAG GG- 3'

Table 2.2 Primers used in real-time PCR

Gene target	Product size (bp)	Sequence	Efficiency (%)
H^+-ATPase	245	F: 5'-TCC CTG ATC TGA CGG GAT AC-3'	101.7
		R: 5'-CGA GGT CAA AGC TTC CTC AC-3'	
NHE3	216	F: 5'-GTG TCA TTT GGA GGC TCG TT-3'	104.7
		R: 5'-ATC CAT GTT GGC GGT AAT GT-3'	
NHE2	206	F: 5'-GAG CGC TGG GAT ACA TTC TC-3'	88.7
		R: 5'- ATT TTC GGC GTA CTG TTT GG-3'	
18s	166	F: 5'-AAA CGG CTA CCA CAT CCA AG -3'	98.4
		R: 5'-CAC CAG ATT TGC CCT CCA-3'	

CHAPTER 3.

Consequences of gill remodeling on Na^+ fluxes and transporter expression in goldfish, *Carassius auratus*

3.1 ABSTRACT

Goldfish adaptively remodel the morphology of their gills when acclimated to conditions that reduce metabolic demand for O_2 (i.e. a normoxic, cold environment) with the growth of a mass of cells, termed the interlamellar cell mass (ILCM), that cover the lamellae. The ILCM decreases the functional surface area of the gills and increases the blood-to-water diffusion distance, presumably in an effort to decrease energetic costs associated with osmoregulation. When acclimated to warmer conditions or lowered ambient O_2 this cell mass is shed, re-exposing the lamellae and increasing branchial surface area, to facilitate an increase in O_2 uptake to match demand. In conditions where the ILCM is present, Na^+ efflux (passive diffusion) was significantly lower in goldfish as was influx (active uptake). There was increase in Na^+ efflux following chronic exposure to hypoxia or after a metabolic recovery in normoxia, despite increased branchial surface area, a result that remains unexplained. Expression of Na^+ transport-relevant genes was not different at either temperature but, Na^+ uptake cells were re-distributed to the edge of the ILCM, presumably in an attempt to maintain contact with the surrounding medium.

3.2 INTRODUCTION

For the gill to function optimally as a respiratory and osmoregulatory organ, the branchial epithelium of FW fish must act as a barrier, restricting the passive loss of ions, while at the same time, allowing free diffusive movement of gases (O_2, CO_2, NH_3) across the gill. The passive movement of small solutes, ions and gases is proportional to the surface area of the gill and inversely proportional to the blood-to-water diffusion distance. O_2 transfer and O_2 consumption (MO_2) are increased with a large gill surface

area (SA). However, passive ion losses are similarly increased (Randall et al., 1972). The conflicting requirements for effective gas transfer and minimal ion loss lead to the so-called 'osmorespiratory compromise' that is though to set an energetic limit on the size of the gill. The energetic costs associated with ion loss stem from the need for their replenishment by ATP-consuming active transport.

Ion uptake across the gill occurs via MRCs found primarily on the filament and to a lesser degree on the lamellae (see Perry, 1997). Na^+ uptake in FW fish occurs against a very steep concentration gradient through one or more pathways (see Evans, 2008), and in exchange for H^+ or NH_3 (NH_4^+) (Maetz and Garcia-Romeu, 1964). The first model describes Na^+ uptake through an electroneutral NHE, which is considered to be thermodynamically unfavorable (see Parks et al., 2008). Numerous studies have however indicated the presence of an NHE in the gill of FW fishes (i.e. Ivanis et al., 2008) and its role in whole animal Na^+ uptake is demonstrated by inhibition of Na^+ uptake to various degrees using amiloride derivatives (NHE channel blocker) (Preest et al., 2005; Esaki et al., 2006). Forward NHE movement is suggested to be possible because of low intracellular concentrations of Na^+ maintained by basolaterally directed movement of Na^+ by numerous Na^+/K^+-ATPase and Na^+-HCO_3^- co-transporters (NBC) that create a 'micro-environment' amenable to Na^+ influx (see Perry and Gilmour, 2006; Hwang, 2009). A second model suggests Na^+ uptake is driven by an electrochemical gradient set up by pumping protons with a V-type H^+-ATPase out of the gill, which favors the inward, passive, movement of Na^+ through an epithelial Na^+ channel (ENaC) (Avella and Bornancin, 1989). A H^+-ATPase model was touted based on immunlocalization in MRCs (Laurent et al., 1994; Lin et al., 1994; Sullivan et al., 1995) and significant

decreases in Na^+ uptake following bafilomycin (H^+-ATPase blocker) (Fenwick et al., 1999) and phenamil (ENaC blocker) exposure (Preest et al., 2005). The caveat is that despite complete annotation of the zebrafish (*Danio rerio*) genome, no gene encoding an ENaC-like protein has been found in any teleost fish. Regardless of the mechanism, reliance on ATPases to drive Na^+ uptake in FW must be energetically costly.

Depending on the osmorespiratory demands, goldfish, along with the closely related crucian carp (*Carassius carassius*), adaptively and reversibly remodel their gills, which can alter functional lamellar surface area and diffusion distance (see Sollid and Nilsson, 2006). Fish acclimated to colder temperatures (< 15°C) exhibit gills that possess a mass of cells termed the interlamellar cell mass (ILCM) that forms between adjacent lamellae, effectively decreasing the surface area of the gill directly exposed to the surrounding water. It is believed that O_2 uptake to meet tissue O_2 requirements is not impeded by the loss of SA accompanying acclimation to cold water because of a decreased metabolic rate and increased solubility of O_2 at low temperatures, accompanied by the presence of a high O_2-affinity hemoglobin in crucian carp (Sollid et al., 2005) and goldfish (Burggren, 1982). Upon exposure of fish to a warmer environment, the metabolic demand for O_2 increases. When O_2 demand surpasses the limitation imposed on O_2 uptake by the dimensions of the gill, the ILCM is shed to increase the surface area of the gill available for gas exchange. The immediate stimulus for remodeling is not known; however, the force directing the change in gill phenotype is suspected to be O_2. Consistent with this idea, shedding of the ILCM can be stimulated through exposure to hypoxia (Sollid et al., 2003), exercise (Fletcher C, Perry SF, Tzaneva V and Gilmour KM, unpublished results) and hypoxaemia (Tzaneva and Perry, 2010).

The goal of this study was to determine the consequences of the ILCM on Na^+ transport across the gill under environmentally relevant stimuli that induce gill remodeling; specifically, remodeling associated with temperature change and hypoxia. In keeping with current models for Na^+ uptake across the gill, it was of particular interest to determine whether ionocytes containing putative Na^+ uptake elements (NHE and H^+-ATPase) are redistributed during gill remodeling to ensure continued contact of the Na^+-transporting ionocytes with the external environment.

3.3 MATERIALS AND METHODS

See Chapter 1

3. 4 RESULTS

Unidirectional Na^+ fluxes

The effect of the ILCM (through thermal gill remodeling) on unidirectional Na^+ fluxes is illustrated in Figure 3.1. It should be noted that a positive value indicates a net inward movement of Na^+ and a negative value indicates a net outward movement of Na^+. No attempt was made to isolate the branchial component of Na^+ influx. However, the contribution of other epithelia such as skin and opercula (Burgess et al., 1998) is negligible in FW fish. Renal contributions to efflux were surgically precluded (see Materials and Methods). There was a significantly greater ($P < 0.05$, student's t-test) rate of Na^+ efflux ($J_{out}Na^+$) in fish lacking an ILCM (25°C acclimated fish; 1275.3 ± 219.0 μmol kg^{-1} h^{-1}) compared to fish with an ILCM (7°C acclimated fish; 650.6 ± 146.8 μmol

kg^{-1} h^{-1}). Correspondingly, there was a significantly higher ($P < 0.05$, student's t-test) rate of Na^+ influx ($J_{in}Na^+$) in the 25°C acclimated group (680.9 ± 67.1 μmol kg^{-1} h^{-1}) compared to the 7°C acclimated fish (360.8 ± 71.3 μmol kg^{-1} h^{-1}). The stress inherent in the surgical procedures may cause efflux values to be slightly exaggerated (when compared to true resting conditions) and the apparent Na^+ imbalance, when comparing measured efflux and influx of Na^+, is likely an artifact of that. Measured net fluxes in 25°C acclimated fish were positive during the 4 h flux period (159.4 ± 94.6 μmol kg^{-1} h^{-1}) and significantly higher ($P < 0.05$, student's t-test) than the net flux measured in the 7°C fish (-95.2 ± 60.7 μmol kg^{-1} h^{-1}). There were no significant differences in plasma [Na^+] between fish at 7 and 25°C (Table 3.1).

Increases in temperature are correlated with increased ventilation rates in fish (Meuwis and Heuts, 1957) that may exacerbate $J_{out}Na^+$ because of increases in external convection of the Na^+-containing media. To assess the potential contribution of ventilatory changes, fish acclimated to 25°C were exposed to acute hyperoxia (4 h) which significantly ($P < 0.05$, student's t-test) decreased ventilation rates (Figure 3.2) from 98.4 ± 3.7 to 47.3 ± 2.5 breaths per minute. While it should be noted that both an increase in ventilation rate and in ventilation amplitude may have an effect on the ionoregulatory physiology of the fish, goldfish have been previously observed to modulate only ventilation frequency when exposed to conditions of increased or decreased environmental O_2 (Tzaneva et al., 2010). The change in ventilation frequency was not associated with a decrease of $J_{out}Na^+$ (Figure 3.3) ($P = 0.724$, student's t-test).

There appeared to be no effect of hypoxia-induced shedding of the ILCM on Na^+ efflux (532.0 ± 183.3 and 605.4 ± 162.6 μmol kg^{-1} h^{-1} in hypoxic and normoxic fish,

respectively) (P = 0.662, student's t-test) or influx (270.6 ± 27.7 and 288.3 ± 34.1 μmol kg^{-1} h^{-1} in hypoxic compared to normoxic fish) (Figure 3.4) (P = 0.713, student's t-test). Net fluxes were significantly different (P < 0.05, student's t-test) between the two groups, with normoxic fish (ILCM present) experiencing a negative net flux (-102.5 ± 42.6 μmol kg^{-1} h^{-1}) and hypoxic fish (ILCM absent) exhibiting a positive net flux (43.4 ± 37.3 μmol kg^{-1} h^{-1}). Following hypoxia exposure, a separate group of 7°C fish was allowed to recover for 12 h in normoxia. As depicted in Figure 3.5, this protocol was without effect on $J_{out}Na^+$ (387.6 ± 42.8 μmol kg^{-1} h^{-1} compared to 289.3 ± 28.9 μmol kg^{-1} h^{-1} for normoxic control) (P = 0.300, student's t-test) or $J_{in}Na^+$ (262.8 ± 33.3 compared to 325.5 ± 114.0 μmol kg^{-1} h^{-1} for normoxic control) (P= 0.622, student's t-test). Fish exposed to hypoxia and then allowed to recover in normoxia experienced a greater negative net flux (-185.8 ± 51.5 μmol kg^{-1} h^{-1}) than corresponding control fish, which were never exposed to hypoxia (-44.7 ± 66.43 μmol kg^{-1} h^{-1}; P = 0.008, student's t-test). Plasma [Na^+] was elevated following hypoxia (Table 3.1).

Expression of putative Na^+ transport genes

Real-time PCR analysis (Figure 3.6) revealed no effect of temperature or ILCM on the branchial expression of NHE2, NHE3 or H^+-ATPase in 7°C acclimated individuals compared to the 25°C group (P = 0.429, 0.167 and 0.318, respectively; student's t-test). There was also no difference in mRNA expression in 7°C fish (Figure 3.7) exposed to hypoxia for 7 days for NHE2 (P = 0.935, student's t-test), NHE3 (P = 0.395, student's t-test) or H^+-ATPase (P = 0.459, student's t-test).

Distribution of Na^+ transport-relevant mRNA in branchial epithelium

In the 25°C goldfish, mRNA expression of transporters presumed to be involved in Na^+ uptake (H^+-ATPase and NHE3) was localized to cells found at the base of the lamellae, in the interlamellar region of the filament and on the lamellae (Figures 3.8A, 3.9A and C for H^+-ATPase; 3.10A and 3.11 A and C for NHE3). Despite its abundance as indicated by real time PCR, I was unable to localize NHE2 mRNA using in situ hybridization. Upon acclimation to 7°C and growth of the ILCM, mRNA for these transporters was expressed in cells on, or close to, the edge of the ILCM, with the occasional Na^+-transporter-rich cell found within the cell mass (Figures 3.8B, 3.9B and D for H^+-ATPase; 3.10B and 3.11B and D for NHE3). These cells appeared to maintain association with the surrounding environment, the lamella or both. Hypoxia exposure (7-days) resulted in the loss of the ILCM and mRNA expression of H^+-ATPase and NHE3 was again largely confined to the filament at the base of the lamellae and on the lamella itself (Figures 3.8C and 3.10C, respectively). Sense probe incubation did not result in any staining for H^+-ATPase and NHE3 (Figure 3.8D and 3.10D, respectively).

3.5 DISCUSSION

The major findings in this study were that 1) there was a coincident decrease in both the efflux and influx of Na^+ in fish with an ILCM 2) branchial Na^+-uptake cells were re-distributed to the edge of the ILCM, (3) Na^+ loss was regulated during hypoxia, despite large increases in branchial SA. (4) Surprisingly, no effect of a metabolic recovery on Na^+ flux was detected despite differences in gill SA at a constant temperature.

As previously observed in other studies (Sollid et al., 2005; Mitrovic et al., 2009; Mitrovic and Perry, 2009), goldfish acclimated to 7°C and 25°C possess gills with and without an ILCM, respectively. Goldfish acclimated to 7°C but exposed to hypoxia also exhibit gills with protruding lamellae (Sollid et al., 2003; Mitrovic et al., 2009). As described in the aforementioned studies, the ILCM gill phenotype is characterized by decreased functional lamellar surface area and increased blood-to-water diffusion distance. The alternative phenotype, lacking an ILCM, is characterized by protruding lamellae, a maximum gill surface area and minimum blood-to-water diffusion distance.

Goldfish with an ILCM resulting from thermal acclimation have reduced efflux* and *influx of Na^+

The decrease in $J_{out}Na^+$ observed in 7°C fish is likely to be attributed, at least in part, to the presence of the ILCM. The approximately 2-fold decrease in Na^+ efflux in 7°C acclimated fish is consistent with the decrease in PEG-4000 (a paracellular marker) efflux observed in goldfish under similar conditions (Mitrovic and Perry, 2009) and supports the notion that the ILCM presents a barrier for diffusive ion loss. To my knowledge, Na^+ fluxes have not been previously examined in cold water-acclimated goldfish and unidirectional efflux measurements have not been made at any acclimation temperature. Na^+ influx rates in 25°C calculated in this study broadly agree with values determined by Preest et al. (2005) on goldfish acclimated to 26°C.

Evaluating the specific role of the ILCM in minimizing diffusive Na^+ loss during thermal acclimation is unavoidably complicated by the potential contribution of a myriad of other temperature-related effects such as increases in external (ventilation) and internal

(perfusion) convection with increasing temperature and increases in thermal energy of the system (Barron et al., 1987). To assess the potential contribution of ventilatory changes to $J_{out}Na^+$, hyperoxia was used as tool to eliminate or minimize convective differences between the two temperature groups. Hyperoxia exposure decreased the rate of ventilation (Figure 3.2) similar to that observed in 7°C acclimated fish (V. Tzaneva and S.F. Perry, unpublished results), without any accompanying changes in $J_{out}Na^+$ (Figure 3.3). Ventilation-independent Na^+ efflux supports the contention that the ILCM is responsible for reducing a significant portion of the observed Na^+ efflux.

Na^+ influx was reduced similar to that of $J_{out}Na^+$ in fish possessing an ILCM, which suggests the existence of an exchange diffusion mechanism for Na^+ uptake or that $J_{in}Na^+$ is decreased to match $J_{out}Na^+$. Considering the stenohalinity of goldfish and their inability to excrete excess Na^+ when exposed to higher environmental salinity, an exchange diffusion mechanism for Na^+ is unlikely because of a limited ability to increase Na^+ efflux in the face of increased external Na^+ concentrations (Lahlou et al., 1969). The more probable explanation is that influx is matched to efflux, which is also consistent with the notion that gill remodeling decreases energetic cost of ion pumping. Active Na^+ uptake, however, may also be subdued by cold acclimation through enzyme inhibition.

Net Na^+ fluxes were negative in fish possessing an ILCM indicating Na^+ loss, while in fish not possessing an ILCM a positive net flux of Na^+ was observed indicating Na^+ gain. When I compared the differences in unidirectional efflux between temperature groups (55%) and the differences in unidirectional influx between temperature groups (47%), it is clear that the ILCM inhibited efflux to a slightly greater degree than influx. The unidirectional flux measurements, using radiotracers, are arguably more accurate

than net flux measurements, which are based on total [Na^+] in the water samples. The net flux measurements in 7°C fish predict a slight negative Na^+ balance, however, not statistically different from zero and reflect the tight matching of Na^+ efflux and influx in fish possessing an ILCM. This is reflected by the constant plasma [Na^+] (Table 3.1) between temperature groups, and suggests full compensation for the decreased branchial SA in 7°C-acclimated fish. Literature data on plasma ion concentrations in goldfish over a wide range of temperatures are highly variable. However, interpolation of the data on goldfish from Murphy and Houston (1973) agrees with constant plasma [Na^+] at the temperatures used in the current study. Many studies report a trend for plasma [Na^+] and [Cl^-] to decrease as temperature decreases (below 10°C) in common carp (Houston and Madden, 1968) and goldfish (Prosser et al., 1970; Catlett and Millich, 1976); Umminger, 1969) while still others reported increases in plasma [Na^+] (Houston and Mearow, 1981) and [Cl^-] (Mitrovic and Perry, 2009) with decreased temperature in goldfish.

Hypoxia limits Na^+ loss despite increase in SA

There was no effect of the cell mass on fish at 7°C (with an ILCM) and hypoxic-remodeled goldfish with protruding lamellae (Figure 3.4). Hypoxic goldfish, however, experience a slightly positive $J_{net}Na^+$ compared to a negative and significantly lower $J_{net}Na^+$ in control 7°C fish, which resulted in significantly higher plasma [Na^+] in hypoxic goldfish compared to normoxic (Table 3.1). This result suggests that hypoxic goldfish are able to regulate gill permeability independent of branchial surface area. A similar phenomenon was reported for Cl^- and PEG, where the authors have suggested a substantial decrease in transcellular and paracellular permeability after hypoxia-

acclimation, despite large changes in branchial surface area (Mitrovic et al., 2009). This phenomenon was also observed in other studies reporting generalized decreases in gill permeability during hypoxia exposure (Hochachka, 1986; Lutz and Nilsson, 2007; Wood et al., 2007; Wood et al., 2009). An increase in plasma [Na^+] following hypoxic exposure is surprising and at this time inexplicable. From these data, goldfish appear to tightly regulate Na^+ loss, preferentially over Cl^-. This observed effect of hypoxia exposure on plasma ions is contradicted by two studies reporting decreases in plasma concentrations of Cl^- in hypoxia remodeled goldfish (Mitrovic et al., 2009) or plasma Na^+ and Cl^- in hypoxia-remodeled Qinghai carp (Matey et al., 2008). The Qinghai carp returned plasma ions to control values after 10 h recovery in a normoxic environment, which coincided with the return of the ILCM, albeit a less dramatic ILCM, suggesting quicker changes in gill morphology in this species than the goldfish or crucian carp (Matey et al., 2008).

Metabolic recovery of hypoxia-acclimated fish does not stimulate Na^+ efflux despite SA difference

A 12 h recovery from chronic hypoxia in a normoxic environment, surprisingly, did not result in a stimulation of Na^+ efflux (Figure 3.5) and was without consequence for the plasma Na^+ concentration. However, net fluxes indicated a significantly larger negative net flux in the recovery fish than in normoxic control fish, which may be indicative of differences in flux attributed to differences in branchial SA. Na^+ efflux must then be regulated to some extent to avoid a significant loss across the gill. Considering the increased surface area of the gill following chronic hypoxia exposure, this result is unexpected (Figure 3.1) and in contrast to a significant efflux in both PEG

and Cl^- following a 12 h recovery in normoxia (Mitrovic et al., 2009). This experiment should provide a true test of the ILCM as a barrier, as there are not any confounding effects from temperature or PO_2 differences (Mitrovic et al., 2009). There is no explanation at this time for the discrepancy in these findings.

Putative Na^+ uptake cells are re-distributed to outer edge of ILCM

There were no significant differences in mRNA expression associated with temperature acclimation or branchial surface area (Figure 2.6). However, there was a re-distribution of cells expressing Na^+-relevant genes. Tightly matching the decrease in Na^+ efflux with influx, without an increase in mRNA expression (although it must be noted that neither protein expression nor transporter activity have been evaluated in this study) is consistent with an energy conservation model at colder temperatures with the goal of conserving energy stores.

In goldfish lacking a branchial ILCM (acclimated to 25°C), cells enriched in NHE3 and H^+-ATPase were localized primarily on the filament epithelium in the interlamellar region or at the base of lamellae (Figure 3.9A, 3.10A and 3.11A, respectively). Acclimation to 7°C stimulated the growth of the ILCM after which this cell type appeared to be re-distributed along the edge of the ILCM (Figure 3.9B, 3.10B, 3.11B, respectively). Probes generated for NHE2 did not produce any staining, despite real-time PCR analysis demonstrating a significant presence; however, it is not likely that cells expressing NHE2 would differ greatly in distribution from those expressing NHE3 or H^+-ATPase, considering the known association of these ion-transporting genes with MRCs in general. The cells at the edge of the ILCM appeared to be oriented in such a

way as to maximize the interaction with either the external environment or with the lamellar epithelium, or both (see Figures 3.10 B and 3.11 C). Transport of Na^+ from the environment, through the ILCM to the circulation has not been examined experimentally, however, is likely to occur via the lamellar circulation, considering the association of these cells with the lamellae. The physiological and molecular identity of the individual cells within the ILCM has also not been investigated, however, it is thought that they are not vascularized and not directly innervated (Nilsson, 2007).

Conclusion

These data demonstrate that there is a decrease in efflux and influx in goldfish acclimated to 7°C (with the ILCM) compared to 25°C (without the ILCM). Although the effect of temperature was considered and external convective processes controlled for, it cannot be ruled out that temperature differences are responsible for the decreased efflux and *not* the ILCM. This observed effect is not conserved in the remodeling of the gill that occurs as a result of chronic hypoxia exposure or following a recovery in 12 h of normoxia. That hypoxia exposure and the increase in gill surface area do not result in greater diffusive efflux of Na^+ is likely the result of non-specific hypoxia effects coordinating a general downregulation of gill permeability. Inexplicably, however, following a metabolic recovery there is still no change in branchial Na^+ flux. The reasons for this will require further investigation. Finally, there is no difference in gene expression of NHE3, NHE2 or H^+-ATPase following temperature acclimation and the cells expressing these genes are re-distributed to the edge of the ILCM where they have access to the surrounding environment.

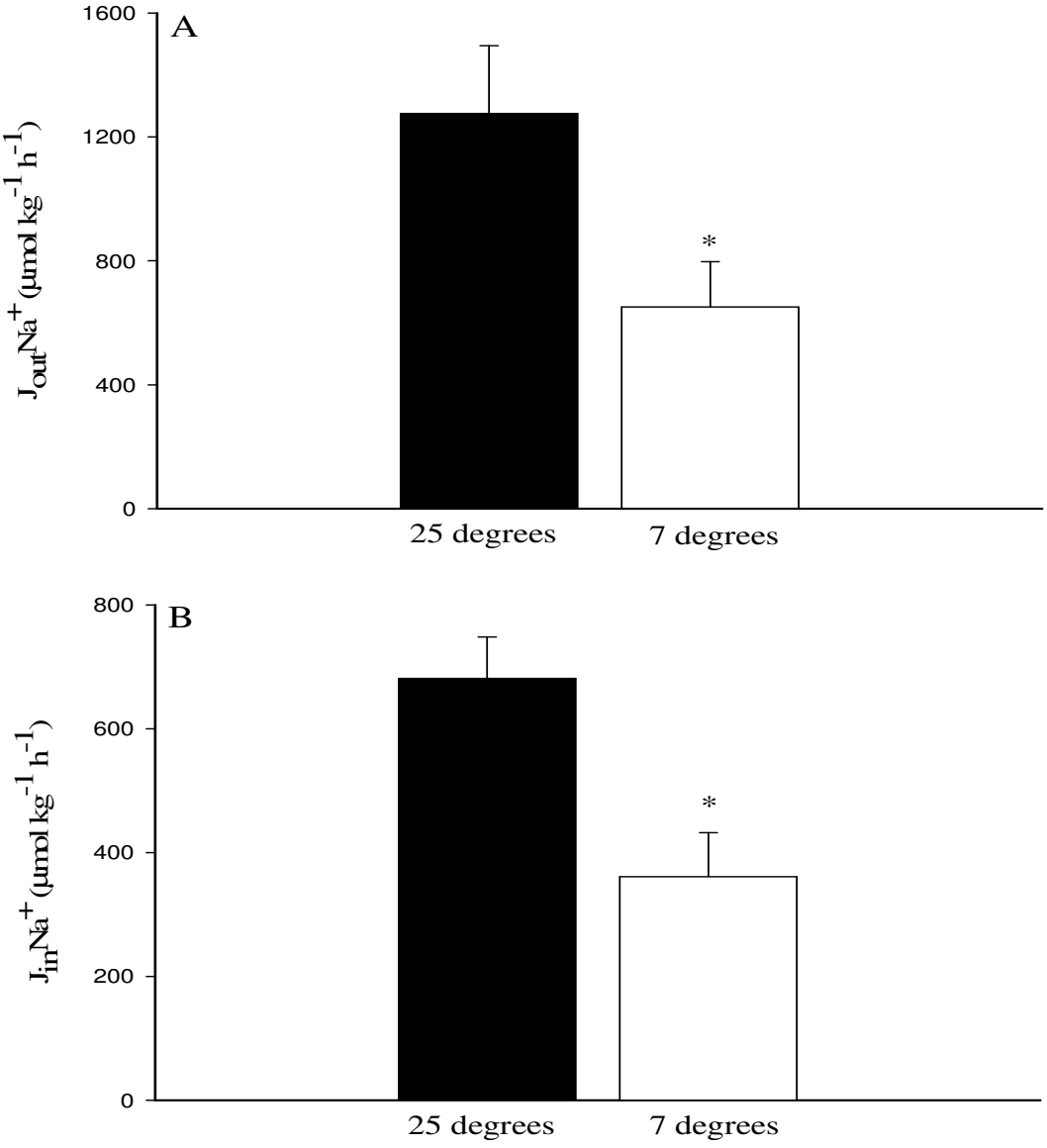
A
1600
1200
800
400
0
$J_{out}Na^+$ (µmol kg^{-1} h^{-1})
*
25 degrees
7 degrees
B
800
600
400
200
0
$J_{in}Na^+$ (µmol kg^{-1} h^{-1})
*
25 degrees
7 degrees

Figure 3.1

Effect of acclimation temperature on branchial (A) Na^+ efflux ($J_{out}Na^+$) and whole-animal (B) Na^+ influx ($J_{in}Na^+$) (filled bars represent 25ºC acclimated goldfish, N = 6; unfilled bars represent 7ºC acclimated goldfish, N = 6). Data are presented as means ± 1 SEM. * represents significant differences between temperature groups ($P < 0.05$; student's t-test).

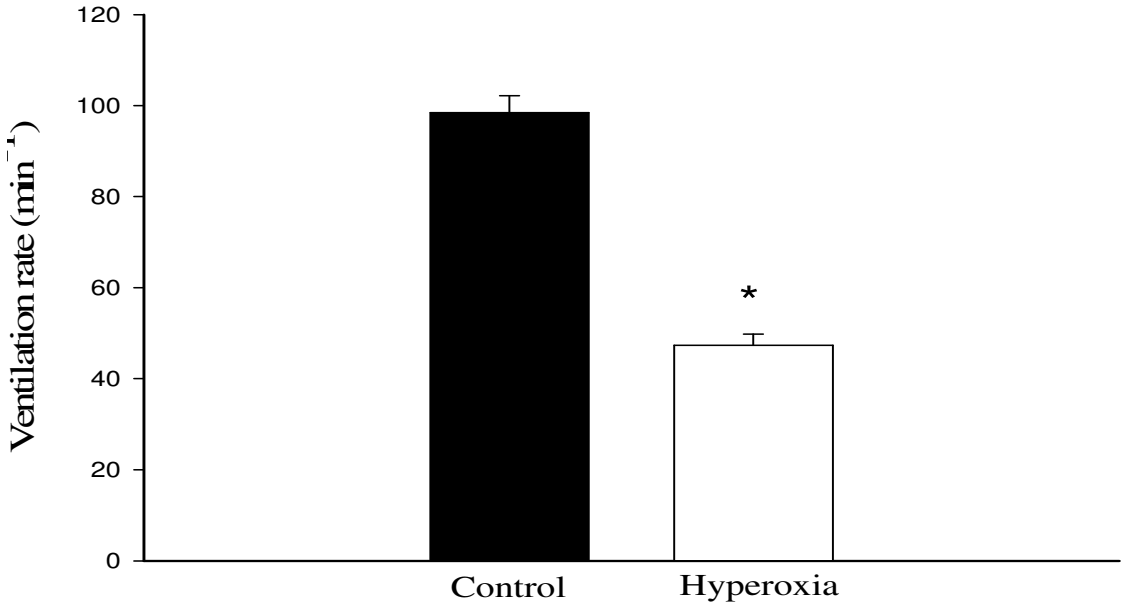
120
100
80
60
40
20
0
Ventilation rate (min-1)
*
Control
Hyperoxia

Figure 3.2

The effects of hyperoxia (PO_2 ~ 400 mmHg) on ventilation frequency in goldfish acclimated to 25°C (N = 4). Filled bars represent normoxic ventilation rates and open bars represent hyperoxia exposed fish. Data are presented as means ± 1 SEM. * indicates statistical significance ($P < 0.05$, student's t-test).

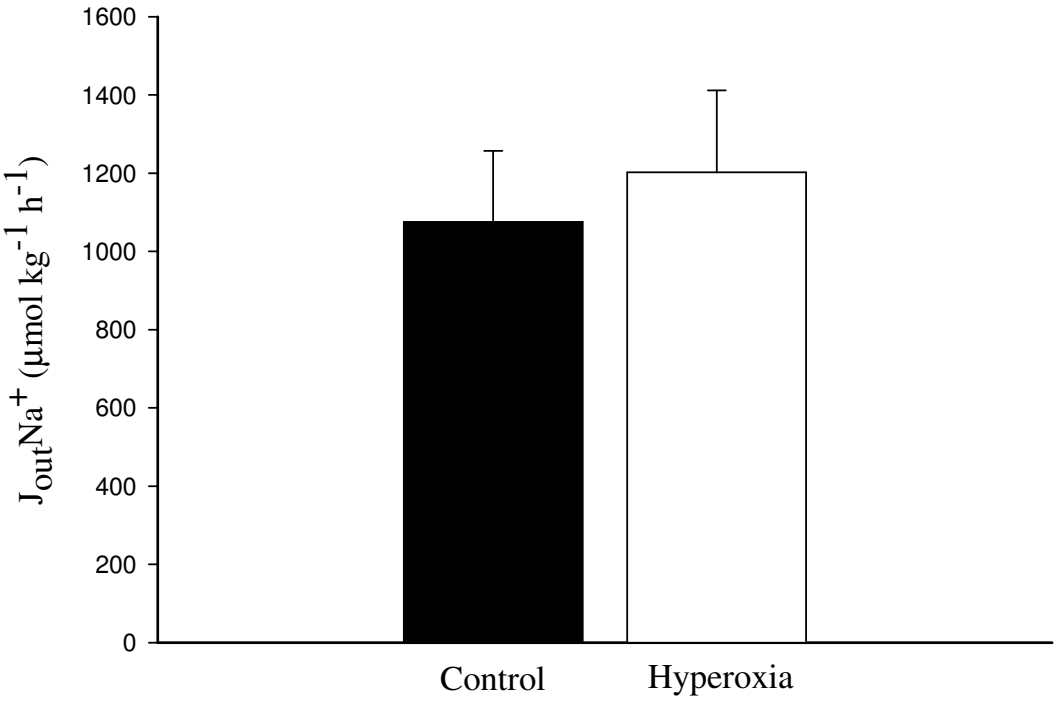
1600
1400
1200
1000
800
600
400
200
0
$J_{out}Na^+$ (µmol kg^{-1} h^{-1})
Control
Hyperoxia

Figure 3.3

The effect of hyperoxia (P_{O2} ~ 400 mmHg) on branchial sodium efflux ($J_{out}Na^{+}$) in goldfish acclimated to 25°C. The filled bars represent control fish exposed to normoxia (N = 6) and unfilled bars represent hyperoxia exposed fish (N = 6). Data are presented as means ± 1 SEM. No significant differences were detected (P = 0.724, student's t-test)

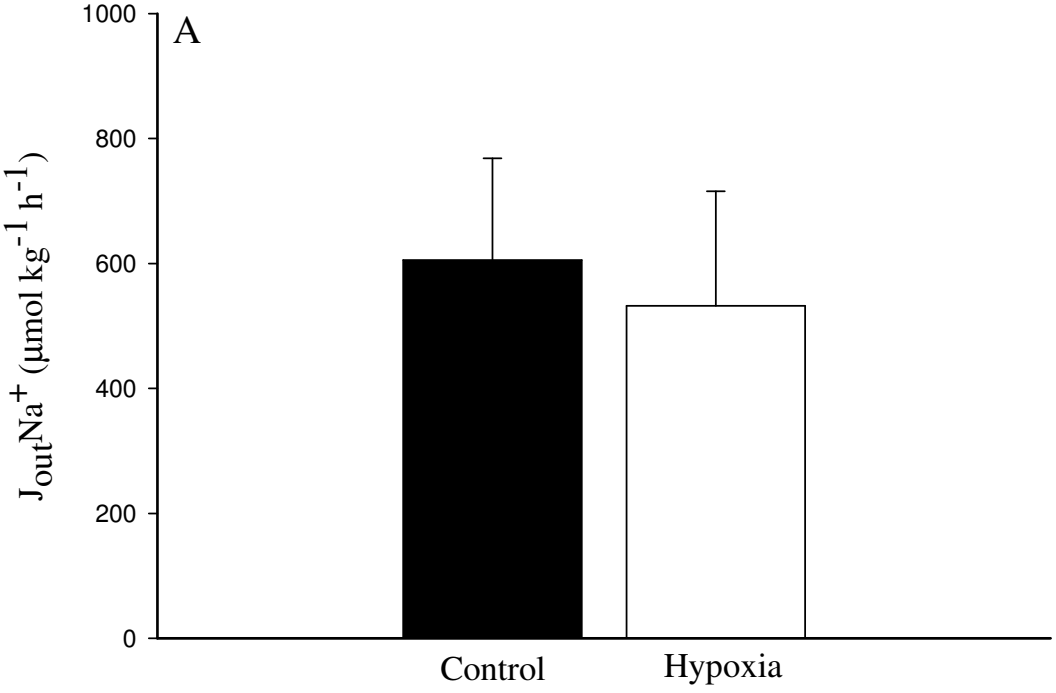
A
1000
800
600
400
200
0
$J_{out}Na^+$ (µmol kg^{-1} h^{-1})
Control
Hypoxia

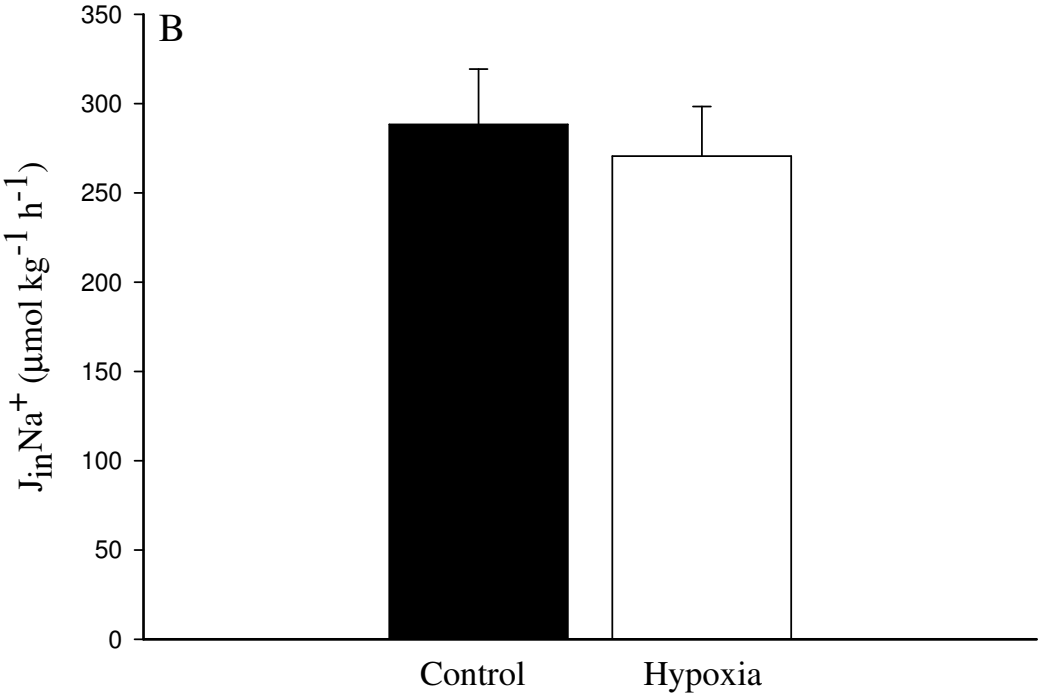
B
350
300
250
200
150
100
50
0
$J_{in}Na^+$ (µmol kg^{-1} h^{-1})
Control
Hypoxia

Figure 3.4

Effect of 7 days of hypoxia exposure on branchial sodium fluxes measured under hypoxic conditions (filled bars represent 7ºC acclimated goldfish exposed to 7 days of hypoxia; unfilled bars represent 7ºC acclimated control goldfish exposed to 7 days of normoxia). (A) Unidirectional sodium efflux ($J_{out}Na^{+}$) (N = 8, N = 6, respectively) and (B) sodium influx (N = 11, N = 6, respectively). Data are presented as means ± 1 SEM. No significant differences were detected in influx (P = 0.713, student's t-test) or efflux (P = 0.662, Mann-Whitney U test).

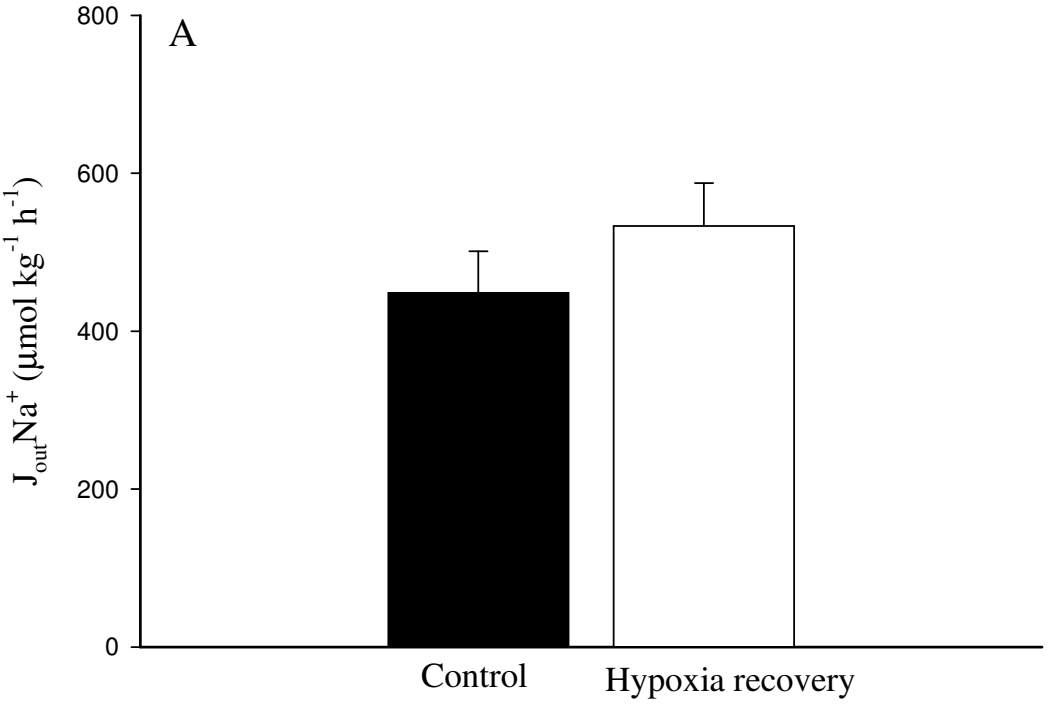
A
800
600
400
200
0
$J_{out}Na^+$ (µmol kg^{-1} h^{-1})
Control
Hypoxia recovery

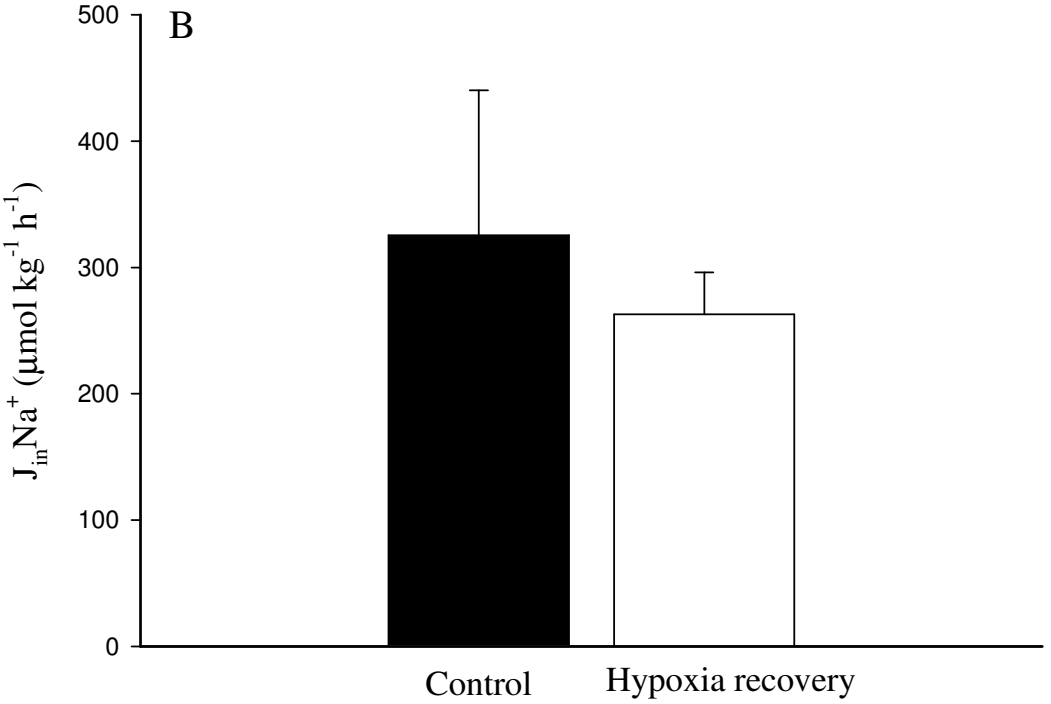
B
500
400
300
200
100
0
$J_{in}Na^+$ (µmol kg^{-1} h^{-1})
Control
Hypoxia recovery

Figure 3.5

Effects of recovery from hypoxia exposure on unidirectional branchial sodium fluxes (filled bars represent 7ºC control goldfish; unfilled bars represent 7ºC hypoxia recovery goldfish, *Carassius auratus*. Recovery fish were exposed to 7 days hypoxia followed by 12 h recovery in normoxic water, control fish were exposed to 7 days normoxia followed by an additional 12 h of normoxic conditions. (A) Unidirectional sodium efflux (N = 10, N =7, respectively) and (B) sodium influx (N = 11, for both). Data are presented as means ± 1 SEM. No significant differences were detected in influx (P = 0.622, Mann-Whitney U test) or efflux (P = 0.300, student's t-test).

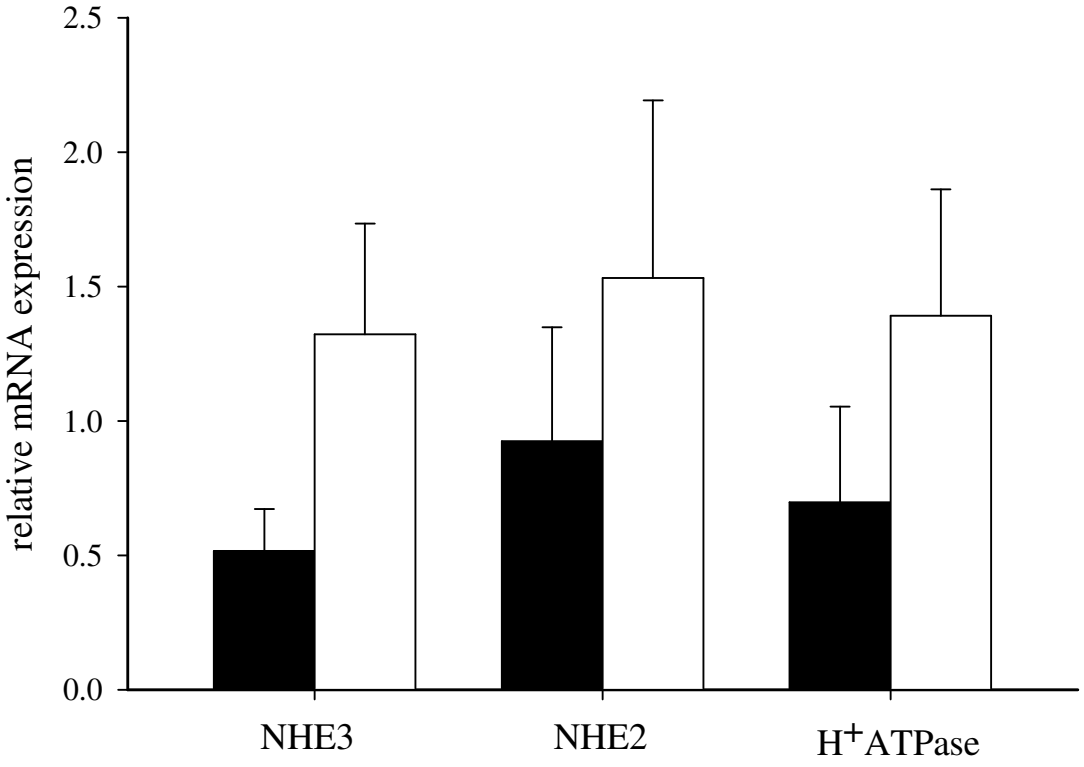
relative mRNA expression
2.5
2.0
1.5
1.0
0.5
0.0
NHE3
NHE2
H+ATPase

Figure 3.6

Effect of temperature acclimation on relative mRNA expression of the Na^+ transport-relevant genes, NHE3, NHE2 and H^+-ATPase. Filled bars represent 25ºC acclimated goldfish, *Carassius auratus*; unfilled bars represent 7ºC acclimated goldfish (N = 4 and N = 3, respectively). Relative expression was calculated by a modified ΔΔ Ct method and is expressed relative to 18S expression and relative to 25ºC acclimated group. Data presented as means ± 1 SEM; * indicates statistical significance ($P < 0.05$, student's t-test).

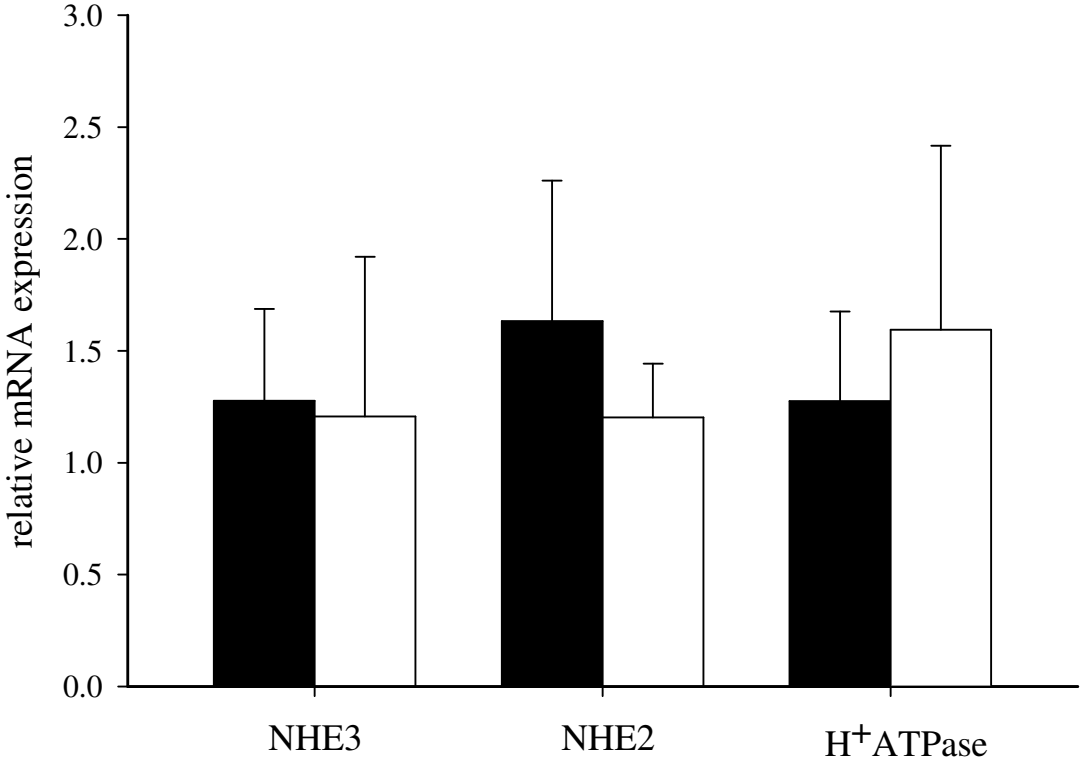
3.0
2.5
2.0
1.5
1.0
0.5
0.0
relative mRNA expression
NHE3
NHE2
H+ATPase

Figure 3.7

Relative mRNA expression of NHE3, NHE2 and H^+-ATPase following chronic (7-day) hypoxia exposure (P_{O2} = 10 mmHg) in goldfish, *Carassius auratus,* acclimated to 7^oC. Filled bars represent normoxic control fish (N = 5) and unfilled bars represent hypoxia exposed fish (N = 6). Data are expressed relative to 18s and presented as means ± 1 SEM. No significant differences were detected (P = 0.935, 0.359, 0.459; student's t-test).

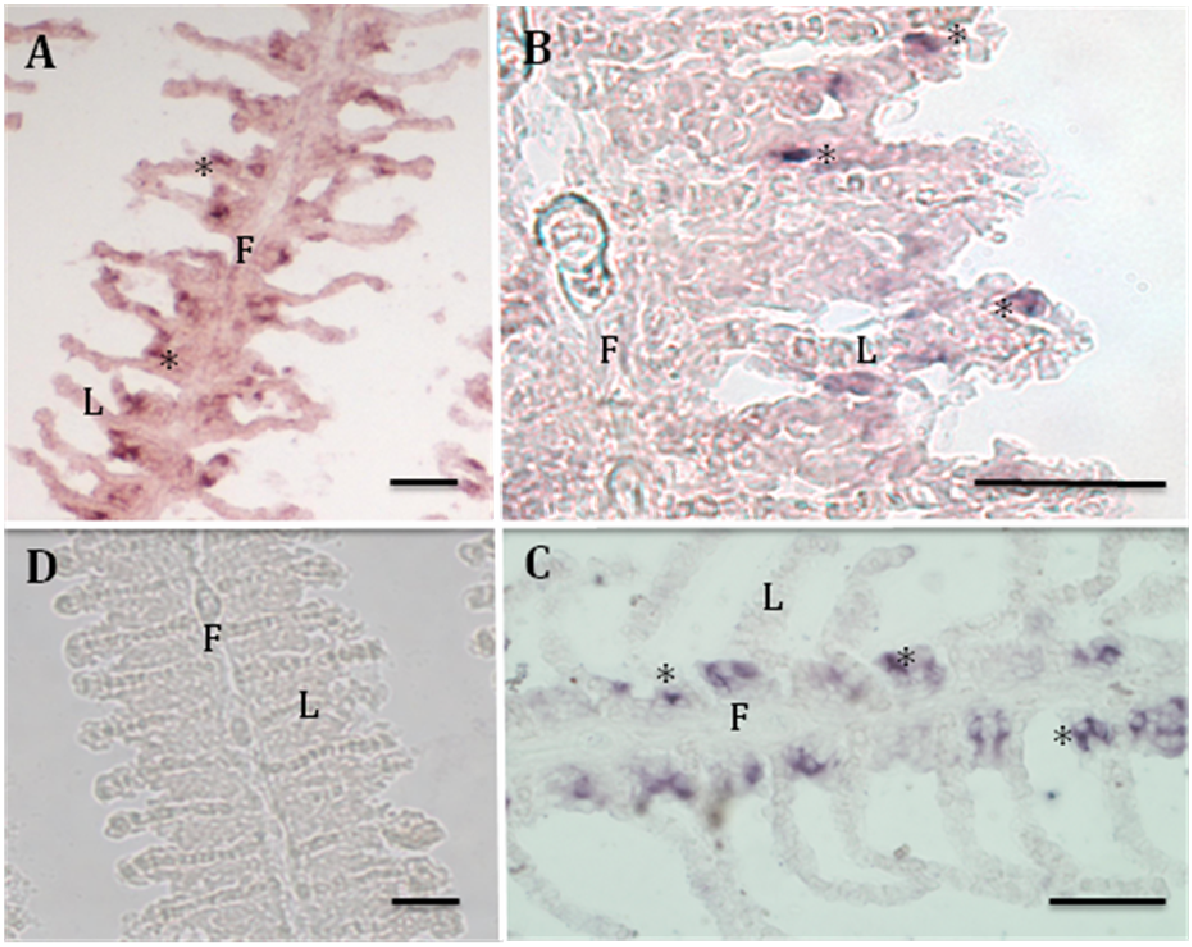

Figure 3.8

In situ hybridization for H^+-ATPase mRNA in the gill of goldfish, *Carassius auratus,* acclimated to 25°C (A), 7°C (B) and after 7-days of hypoxia exposure (~10 mmHg) (C). Hybridization carried out using a sense probe is included in (D). Symbols represent (F) filament, (L) lamellae; * indicates example of cell in contact with lamellar epithelium. Scale bars represent 50 μm.

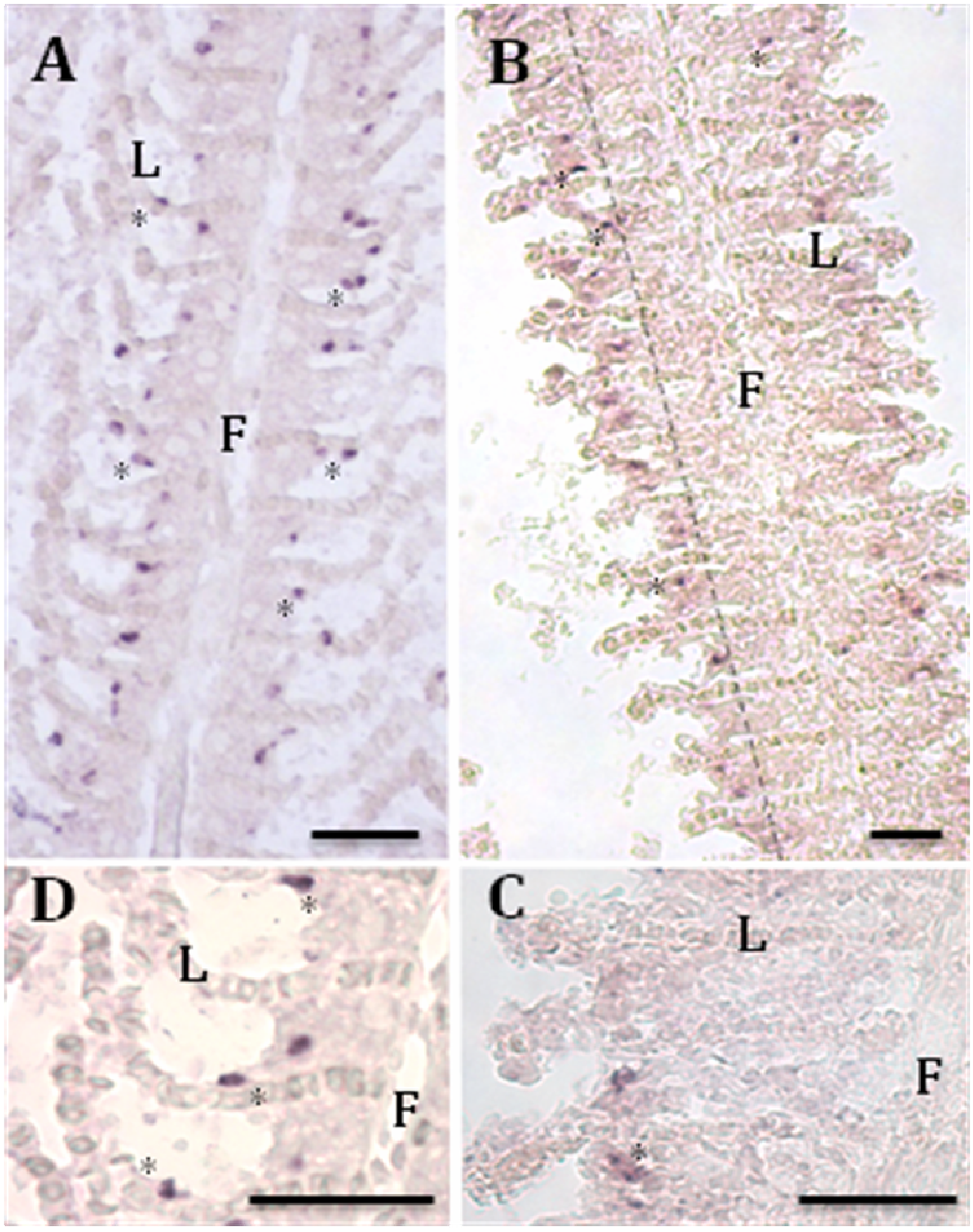

Figure 3.9

Alternate view of branchial H^+-ATPase mRNA expression as viewed by *in situ* hybridization in goldfish, *Carassius auratus*, acclimated to 25°C (A) and 7°C (B) at 10X magnification. Higher (40X) magnification of H^+-ATPase mRNA *in situ* hybridizations in 25°C goldfish gill (C) and 7°C (D). Symbols represent (F), lamellae (L); * indicates example of stained cell in contact with lamellar epithelium. Scale bars represent 50 μm. Dotted line (----) in B represents the innermost limit of stained cells within the ILCM.

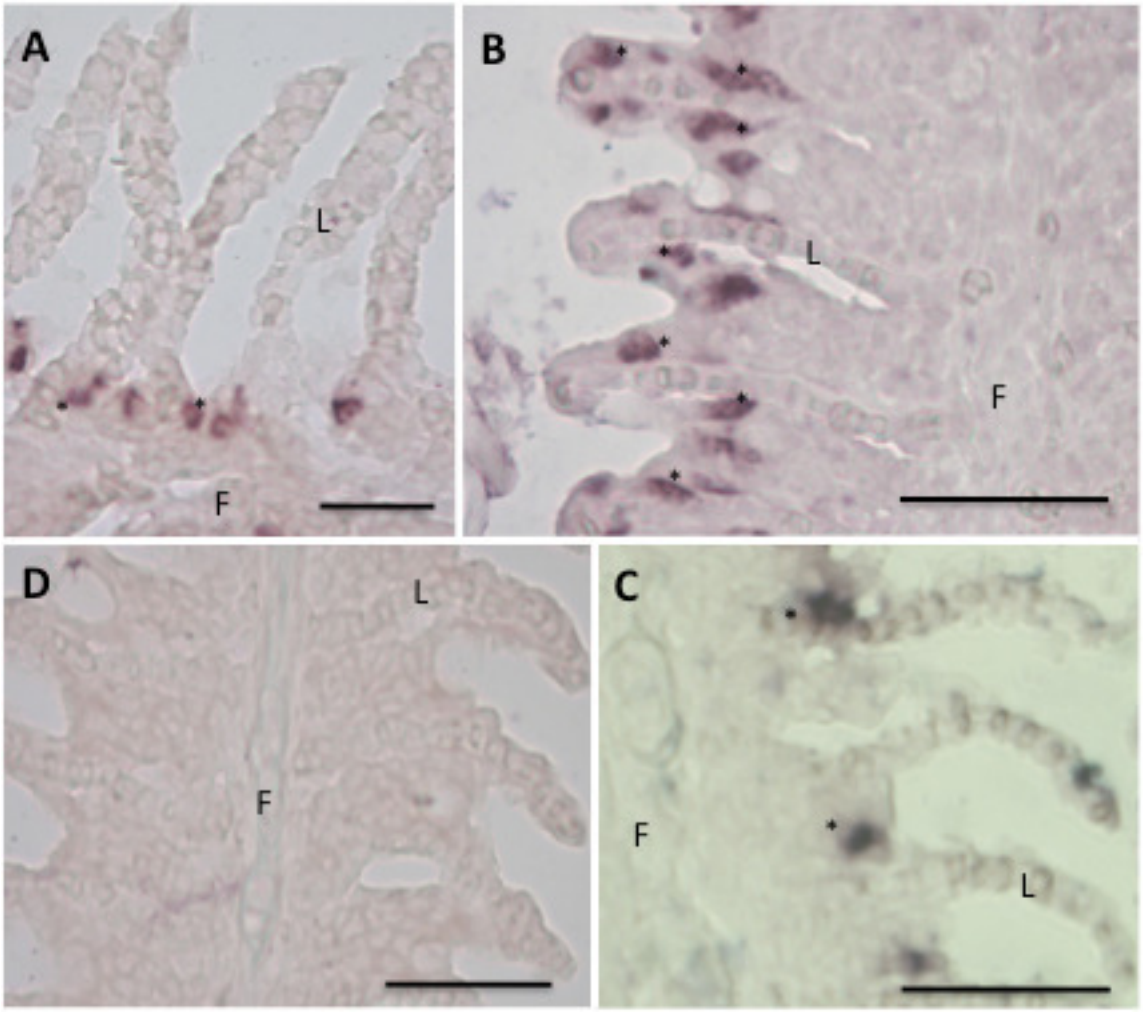

Figure 3.10

Distribution of NHE3 mRNA expressing cells in gills of goldfish, *Carassius auratus,* acclimated to 25°C (A), 7°C (B) and 7°C after 7-days of hypoxia exposure (~10 mmHg) (C). Sense probe for *in situ* hybridization control is included in (D). Symbols represent filament (F), lamellae (L); * indicates example of stained cell in contact with lamellar epithelium. Scale bars represent 50 μm.

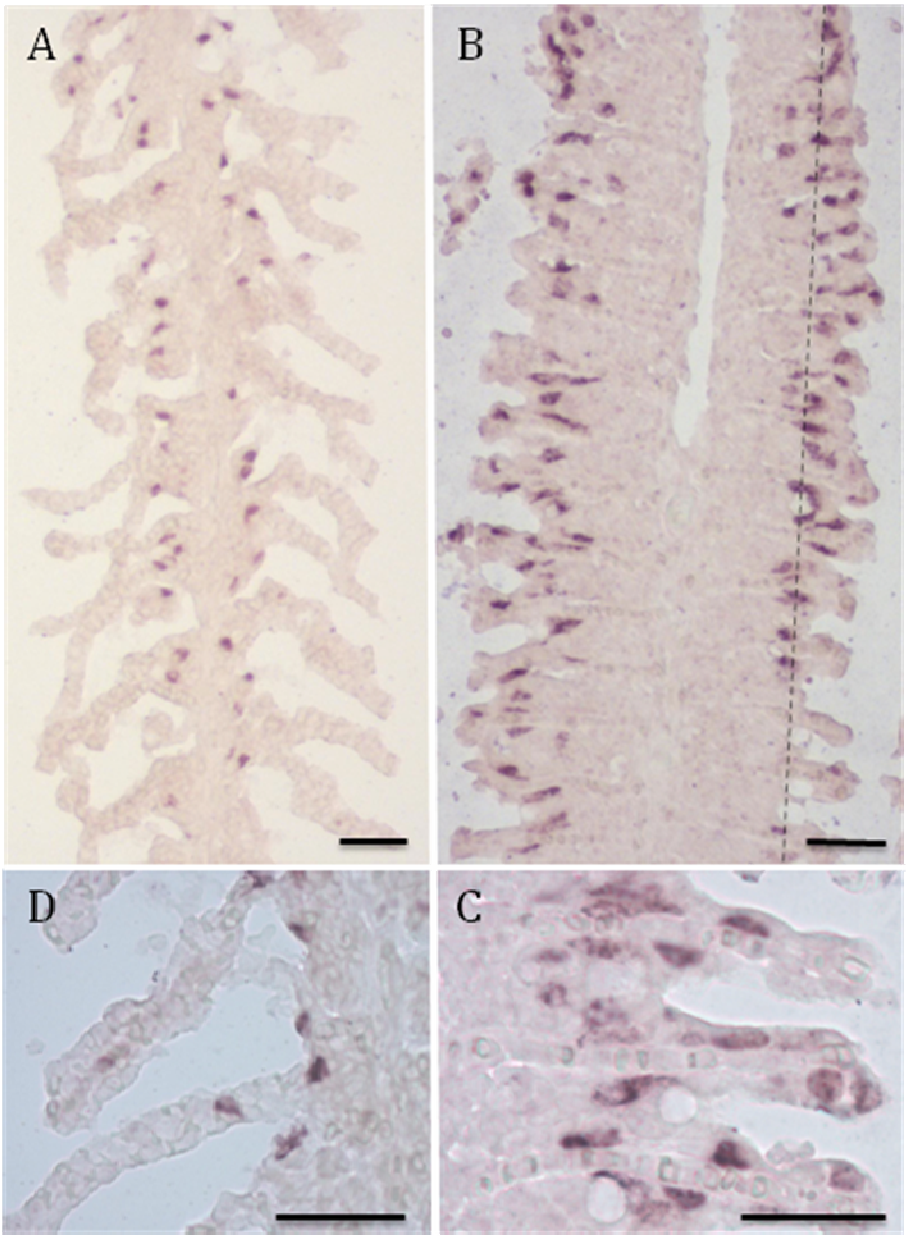
A
B
D
C

Figure 3.11

Alternate view of goldfish gill acclimated to 25°C (A) and 7°C (B) illustrating staining of branchial NHE3 mRNA-rich cells. Images at a higher magnification of 25°C and 7°C are portrayed in (C) and (D), respectively. Symbols represent filament (F) and lamellae (L); * signifies stained cells in contact with lamellar epithelium. Scale bars represent 50 μm.

Table 3. 1. *Effect of gill remodeling on ionoregulatory status of plasma Na^+ values*

	25°C-acclimated	**7°C-acclimated**	**Normoxia**	**Hypoxia**	**Recovery**	**Hyperoxia**
Plasma ion concentration (mmol L^{-1})						
Na^+	121.1 ± 7.0	141.8 ± 7.9	122.5 ± 8.1	146.9 ± 6.4*	140.3 ± 6.4	123.7 ± 3.1

CHAPTER 4.

The effect of gill remodeling on acid-base regulation in goldfish, *Carassius auratus,* exposed to environmental hypercapnia

4.1 ABSTRACT

Goldfish reversibly remodel their gills through the growth or loss of a mass of cells found between adjacent lamellae (interlamellar cell mass; ILCM). The presence of the ILCM is thought to decrease passive ion loss and the costs of osmoregulation when fish are acclimated to a cold (<15^{o}C), normoxic environment. Given the inherent relationship in freshwater (FW) fish between Na^+ and Cl^- uptake and acid-base regulation, the effect of gill remodeling on the ability of fish to compensate respiratory acidosis (elicited by environmental hypercapnia) was assessed. This study revealed that the presence of the ILCM places limitations on the ability of fish to excrete acid equivalents to the environment. There was no effect on blood pH regulation during hypercapnia, however the amount of HCO_3^- accumulated in the blood of 7°C fish (with an ILCM) was not matched by the amount of H^+ excreted to the environment. It is suggested, although not experimentally determined, that the "extra" HCO_3^- found in the plasma was the result of H^+ transfer to intracellular compartments. The similarities and differences in the mechanisms of acid-base regulation in goldfish with and without an ILCM are discussed.

4.2 INTRODUCTION

Acid-base disturbances in fish are corrected through metabolic adjustments at the gill involving excretion of acid equivalents (H^+, NH_4^+) or uptake of basic equivalents (HCO_3^-). Increases in environmental PCO_2 disrupt acid-base homeostasis as a result of the hydration of additional CO_2 and subsequent dissociation of carbonic acid ($CO_2 + H_2O \rightarrow HCO_3^- + H^+$). The blood systemic response to a respiratory acidosis is characterized

by an increase in P_aCO_2, resulting in a decreased blood pH which is followed by a gradual recovery that is achieved by the excretion of H^+ (coupled to Na^+ uptake) and/or uptake of HCO_3^- (coupled to Cl^- excretion). Differential uptake of Na^+ and Cl^- via gill ionocytes then regulates blood pH. Carp have been shown to rely primarily (an approximately 75% contribution) on adjustments in Cl^-/HCO_3^- exchange to regulate pH (Claiborne and Heisler, 1984), whereas the brown bullhead catfish rely equally on Na^+/H^+ and Cl^-/HCO_3^- exchange (Goss et al., 1992a). The freshwater eel (*Anguilla anguilla*), without a capacity for Cl^- uptake, relies solely on Na^+/H^+ exchange (Sherratt, 1964). The mechanism of acid-base regulation in goldfish has not been elucidated; however, given the close phylogenetic relationship between carp and goldfish, it is reasonable to assume (at least as a starting point) that the mechanism of acid-base regulation would be similar.

It follows that an effect of the ILCM on ion flux may also affect the ability to regulate ion fluxes and maintain acid-base homeostasis in the face of a disturbance. Na^+ uptake was decreased in fish possessing an ILCM (see Chapter 3), while Cl^- uptake was not impeded (Mitrovic and Perry, 2009). This study investigated the ability of goldfish to regulate blood pH during environmental hypercapnia in fish acclimated to 7°C (ILCM present or 25°C (LCM absent).

4.3 METHODS

See Chapter 2

4.4 RESULTS

Blood pH response not affected by the ILCM

Exposure to environmental hypercapnia resulted in a significant drop in blood pH in both temperature-acclimated groups. This initial acidosis reached its maximum (within the time frame of the measurements) by 0.5 h in the 25° fish and by 3 h in the 7°C fish (Figure 4.1A). A gradual recovery of pH back to near-normocapnic values occurred over the 48 h exposure period in both groups of fish. While the absolute values of pH were significantly different in the two groups of fish, with the pH of warm-acclimated goldfish being significantly lower than that of cold-acclimated fish, the pattern of pH changes during hypercapnia were similar (Figure 4.1A). The near-restoration of blood pH during hypercapnia was accomplished through the accumulation of HCO_3^- in the plasma (Figure 4.1B). Although absolute values differed significantly between the two groups, the rate of bicarbonate accumulation in the plasma was not different (Figure 4.1B). The pH recovery was incomplete after the 48 h exposure period in both groups of fish, as the pH at all time points was significantly different from the pre-hypercapnic control ($P \leq 0.001$).

Acid excretion to the water

Fluxes of ammonia ($J_{net}Amm$), TA ($J_{net}TA$), H^+ ($J_{net}H^+$) (Figure 4.2) and Na^+ ($J_{in}Na^+$) (Figure 4.3) were measured for both temperature groups during the 48 h period of CO_2 exposure. In all cases, $J_{net}Amm$ occurred in the outward direction (from fish to water). Ammonia excretion was not different between groups, despite the temperature difference ($P = 0.946$) (Figure 4.2A). After the onset of hypercapnia, there was a

significant increase in J_{net}Amm in the 25°C group from 479.3 ± 59.9 to 675.1 ± 79.6 μmol kg^{-1} h^{-1}, returning to pre-hypercapnic efflux rates after 3 h and decreasing to below control values after 24 h ($P < 0.001$). Conversely, the 7°C group did not experience an increase in J_{net}Amm at any point during the exposure, maintaining constant rates until 24 h when J_{net}Amm decreased to lower than control values ($P < 0.001$, 2 way repeated measures ANOVA) (Figure 4.2A). In the 25°C fish, $J_{in}Na^+$ exhibited the same trend as J_{net}Amm; an initial increase in Na^+ influx immediately following the onset of hypercapnia ($P < 0.001$, 2 way repeated measures ANOVA). The increase in Na^+ uptake was maintained until 6 h ($P < 0.05$, 2 way repeated measures ANOVA) and then decreased to values significantly lower than during the normocapnic control period after 24 h ($P < 0.01$, 2 way repeated measures ANOVA) (Figure 4.3). J_{net}TA in 25°C-acclimated fish was negative (indicating net base excretion) until 9 h of hypercapnia exposure at which time there was a net excretion of acid that persisted for the remainder of the hypercapnia exposure (Figure 4.2B). The resulting $J_{net}H^+$ was positive (indicating acid excretion) throughout the entire 48 h period, significantly elevated from pre-hypercapnic control at 9 h (from 214.2 ± 90.6 to 722.8 ± 119.4 μmol kg^{-1} h^{-1}) and decreasing, but remaining significantly elevated from control period until 48 h exposure ($P < 0.05$, 2 way repeated measures ANOVA) (Figure 4.2C). In 7°C acclimated fish there was no effect of CO_2 exposure on J_{net}TA (Figure 4.2B) or $J_{in}Na^+$ (Figure 4.3) over the 48 h period. Despite experiencing no change in J_{net}Amm or J_{net}TA, there was a cumulative, but transient increase in $J_{net}H^+$ in 7°C fish at 6 h ($P < 0.01$, 2 way repeated measures ANOVA), after which the rate of H^+ flux returned to normocapnic values for the remainder of the 48 h period (Figure 4.2C). Subsequent analysis of the change in $J_{net}H^+$ from the pre-

hypercapnic control over the 48 h period between both groups of fish revealed no significant difference between the absolute amounts of H^+ excretion to the water (63.5 ± 17.8 μmol in the 7°C group compared to 104.8 ± 37.2 μmol in the 25°C fish, P = 0.328, student's t-test) (Table 3.1). Assuming a 70% "HCO_3^- space" (Perry et al., 2010), I estimated that HCO_3^- accumulation in the blood amounted to 120.6 ± 42.9 μmol in 25°C goldfish and 131.1 ± 31.9 μmol in 7°C fish by 48 h (P = 0.386, student's t-test) (Table 3.1). The amount of acid added to the external medium accounted for the HCO_3^- accumulation in 25°C fish (P = 0.171, student's t-test). The amount of H^+ excretion to the water in 7°C acclimated fish (with an ILCM), however, was not sufficient to account for the plasma HCO_3^- accumulation (P < 0.05, student's t-test).

Expression of NHEs in 7°C acclimated goldfish increase with CO_2 exposure

Expression of NHE2, NHE3 and H^+-ATPase mRNA in the gills after 48 h of hypercapnia is depicted in Figure 4.4. NHE2 and H^+-ATPase expression were significantly increased in 7°C acclimated goldfish (w/ ILCM) exposed to 48 h CO_2 (~10 mmHg) compared to 7°C control goldfish (P < 0.05, student's t-test) (Figure 4.4A). There was no effect of CO_2 exposure on NHE3 expression in either 7°C or 25°C acclimated groups (P = 0.818 and 0.369, respectively; student's t-test) (Figures 4.4A and B). In 25°C acclimated fish, without branchial ILCM, H^+-ATPase expression was increased (P < 0.05, student's t-test) after 48 h CO_2 exposure, while NHE2 and NHE3 expression were unchanged (P = 0.072 and 0.369, respectively; student's t-test) (Figure 4.4B). There was no observed effect of temperature on gene expression of NHE3, NHE2

and H^+-ATPase in fish exposed to 48h CO_2 (P = 1.00, 0.152 and 0.936, respectively; student's t-test) (Figure 4.4C).

4.5 DISCUSSION

The ILCM delays the impact of an acidosis without affecting recovery of blood pH

The blood pH response in goldfish exposed to CO_2 for 48 h did not differ between fish acclimated to 7°C and 25°C. Although the absolute values of blood pH and plasma [HCO_3^-] differed (Figure 4.1) because of the temperature dependency of pH (Reeves, 1977), the rates of pH recovery and HCO_3^- accumulation were independent of temperature and presence of the ILCM. Neither group achieved complete recovery of pH by the end of the 48 h period. The duration of the recovery period appears to be keyed to the salinity of the environment (Iwama and Heisler, 1991) and the extent of the acidosis (determined by the severity of the hypercapnia) (Claiborne and Heisler, 1986). The current results agree, at least qualitatively, with the classical blood response to respiratory acidosis; other reports of hypercapnia exposure in teleosts have ranged from 8 h to 72 h for complete restoration of pH (e.g. Heisler et al., 1976; Cameron, 1980; Perry et al., 1981). The ILCM appears to have an effect on the initial acidification of the blood after CO_2 exposure is initiated. The maximum acidosis was reached (at least as could be determined with the blood sampling protocol employed) by 0.5 h in 25°C fish and 3 h in 7°C fish. The ILCM may be limiting CO_2 diffusion to the blood and slowing the rate of the acidosis. Indeed, diffusion limitations of CO_2 imposed by the ILCM in cold temperatures have been previously demonstrated in goldfish (V. Tzaneva, K.M. Gilmour and S.F. Perry, unpublished results).

The ILCM affects the time-course of acid-base relevant exchanges with the environment

There was no attempt to separate renal and branchial components of the acid-base regulatory response. Assuming a urine filtration rate (UFR) of 3.31 mL kg^{-1} h^{-1} and 16.17 mL kg^{-1} h^{-1} in cold and warm acclimated goldfish, respectively (Isaia, 1972) (0.06 μM urine [H^+]; 0.58 mM [NH_4^+]) under control conditions (King and Goldstein, 1983) and a 57% increase in urine flow rate in response to acid exposure (0.144 μM [H^+]; 0.76 mM [NH_4^+]) (King and Goldstein, 1983), total H^+ excretion from the kidney amounts to less than 1% whole body H^+ excretion, and thus the contribution of the kidney to net acid excretion can be considered negligible.

The change in pH over the exposure period was similar in both temperature groups (decreased by approx 0.3 pH units). The total amount of bicarbonate accumulated in the plasma appeared to be independent of the ILCM and temperature ($P = 0.62$, student's t-test), as was the amount of H^+ excreted to the environment ($P = 0.39$, student's t-test) (Table 4.1). However, the amount of HCO_3^- accumulated in the plasma could be accounted for the by excretion of H^+ to the environment in 25°C-acclimated fish only (Table 4.1). The non-bicarbonate buffer capacity is relatively small in the blood and likely cannot explain the increase in pH (Heisler, 1984). A possible explanation for the similar HCO_3^- accumulation in the cold-acclimated fish despite an apparently inadequate excretion of acid is the transfer of H^+ to intracellular compartments, the most likely candidate being the muscle. Several studies have reported significantly greater decreases in the intracellular pH of white muscle (compared to blood and other tissues), e.g. lemon sole (*Parophrys vetulus*) (Wright et al., 1988) and spotted dogfish (*Scyliorhinus stellaris*)

(Heisler and Neumann, 1980). H^+ is thought to be sequestered into the tissues and eventually excreted via the gills and/or kidney over a prolonged period in elasmobranchs (Heisler and Neumann, 1980) and freshwater catfish (Cameron, 1980), so it is not unreasonable for the "missing" H^+ excretion in the cold-acclimated goldfish to have occurred after the 48 h time frame of these experiments.

The differences in acid-base regulation in goldfish with and without an ILCM support the hypothesis that the ILCM prevents the movement of Na^+ (or perhaps ions in general) across the gill. Whatever effect the ILCM has on ion movements across the gill, it is without consequence on the blood acid-base status, which was regulated similarly independent of ILCM status. H^+ retention in the ICF, however, may have unwanted consequences on muscle function and/or a delayed recovery following return to normocapnia. Ultimately, eliminating the total acid-load to the water is essential for complete whole body acid-base compensation.

Mechanism of acid excretion is altered by the ILCM

The mechanism of acid-excretion in warm-acclimated fish appears to be biphasic. The earlier component of the acid-excretion appears to be dominated by Na^+/NH_4^+ (H^+) exchange (Figure 4.2 and 4.3) in fish without an ILCM. The form of ammonia excretion (ionized or un-ionized) cannot be discerned from these methods, and therefore these results are also consistent with the Rh model of ammonia excretion (Wright and Wood, 2009). Previous studies involving NH_4^+ injections in goldfish resulted in stimulated Na^+ uptake (Maetz and Garcia Romeu, 1964; Maetz, 1972) and the authors concluded that Na^+/NH_4^+ and Na^+/H^+ exchange both occur depending on the availability of the counter-

ion. The data from the current study are consistent with this view, where Na^+ uptake and NH_4^+ excretion rates are increased coincidentally following the onset of hypercapnic acidosis. The change in Na^+ uptake from control was exceeded by change in ammonia excretion, suggesting that all Na^+ uptake occurred by $Na^+/NH_3(NH_4^+)$.

The majority of the acid load was lost to the environment after ammonia excretion had fallen to pre-hypercapnic rates (Figure 4.2A) at approximately 9-12 h post-hypercapnia exposure, and was not linked to Na^+ transport as a counter-ion (Figure 4.3). Given reports that the primary mechanism of acid-base regulation in common carp was determined to be Cl^-/HCO_3^- exchange (Claiborne and Heisler, 1984), it is likely that the reduction of the acid-load in goldfish is also primarily achieved by a reduction in branchial Cl^-/HCO_3^- exchange. I was unable to measure Cl^- fluxes due to the global unavailability of a commercial supply of Cl^- isotope and so this could not be confirmed experimentally.

The mechanism of acid excretion/base uptake observed in warm-acclimated goldfish without an ILCM is clearly different to that of cold-acclimated goldfish with an ILCM. There was no correlation between Na^+ uptake (Figure 3.3) and ammonia excretion (Figure 3.2A) in cold-acclimated goldfish. The lack of increase in ammonia excretion in cold-acclimated fish (with an ILCM) is curious. If molecular ammonia is excreted by the goldfish, there should be no impediment by the ILCM as inert gases (i.e. oxygen) and small solutes (i.e. ethanol) (Tzaneva V., Perry S.F., Gilmour K.M., unpublished results) appear to freely diffuse across the ILCM. In fact, Maetz (1972) demonstrated that ammonia efflux was driven by partial pressure gradients of NH_3 under low pH conditions only, not under normal pH conditions, suggesting that excretion in the

gaseous state might be predominant under these circumstances. Assuming the mechanism of ammonia excretion is not different in warm and cold acclimated fish, an increase in ammonia excretion in 7°-acclimated goldfish, with already very high basal ammonia excretion rates, may not be possible with the imposition of the cell mass and the decrease in available gill surface area. By any account, the mechanism of acid excretion to the water in fish at 7°C (with ILCM) and 25°C (no ILCM) are clearly different. Without any temperature-related differences to explain these differences, excretion of acid-equivalents must be inhibited by the ILCM. Despite no increases in ammonia excretion in the current study, a spatial redistribution of Rh proteins, thought to act as channels for molecular ammonia transport, within the ILCM has been demonstrated which suggests that this pathway may still be used for ammonia transport in goldfish acclimated to cold temperatures (Perry et al., 2010).

mRNA expression of Na^+-transport proteins increases following CO_2-exposure

The expression of H^+-ATPase increased considerably in 25°C goldfish exposed to hypercapnia (Figure 3.5A) with no change in NHE3 expression and a non-significant increase in NHE2 expression ($P = 0.072$). An increase in branchial H^+-ATPase would clearly improve acid excretion at the gill. Similarly, in 7°C-acclimated goldfish, there was a significant increase in NHE2 and H^+-ATPase expression, with no effect on NHE3 expression (Figure 3.5A). There were no differences in expression when a comparison was made between acid-exposed fish at 7°C and 25°C (Figure 3.5B), which was expected considering the similarity in mRNA expression of these transporters under control conditions (see Chapter 2, Figure 2.6). Increased Na^+-transporter gene expression is

surprising in cold-acclimated fish considering their apparent non-reliance on Na^+ transport-mediated acid-excretion following an acid disturbance. These results may suggest that increases in NHE2 and H^+-ATPase are a generalized temperature-independent response to hypercapnia in goldfish, without any apparent benefit to acid-excretion in cold-acclimated fish – changes to ATPase activity and/or protein expression may be needed to confirm the role, if any, played by H^+ATPase in cold-acclimated goldfish exposed to CO_2.

To my knowledge, no studies have evaluated gene expression in goldfish exposed to an acid-disturbance; however, in rainbow trout exposed to hypercapnia there was a significant increase in NHE2, but not NHE3 mRNA expression (Ivanis et al., 2008), suggesting it as the predominant, acid-excretion Na^+/H^+ exchange isoform. In zebrafish, NHE3b expression is increased in low-Na^+ environments and decreased in low pH environments, further suggesting the role of NHE3 as a Na^+-uptake isoform (Yan et al., 2007) and NHE2 as an acid-excretion isoform. H^+-ATPase mRNA expression was also significantly increased in zebrafish exposed to low pH (Yan et al., 2007), and H^+-ATPase protein was increased in rainbow trout exposed to hypercapnia (Sullivan et al., 1995) and dogfish (*Squalus acanthias*) exposed to low pH (Tresguerres et al., 2005), implying a role for this protein in acid-base regulation.

Conclusion

The results of the present study indicate that there are profound differences in the mechanism of acid excretion following exposure to hypercapnia in goldfish acclimated to 7°C (with an ILCM) and 25°C (without an ILCM). However, their differences appear to

be without consequence for the regulation of systemic pH. The ILCM appears to slow down the inward movement of CO_2 following the initiation of hypercapnia, which is consistent with the diffusion limitations of CO_2 in goldfish acclimated to 7°C (Tzaneva V, Perry SF and Gilmour KM, unpublished results). The recovery of pH following an acidosis occurs to a similar extent and on equivalent time scales between the two temperature groups, but this was not reflected in an equivalent excretion of acid. Given that the accumulation of HCO_3^- in 7°C acclimated fish exceeded the acid H^+ excretion to the water in this 48 h time frame, the extra HCO_3^- must be attributed to H^+ transfer to intracellular compartments, the white muscle being the most likely candidate. *If* that is the case, goldfish acclimated to 7°C would likely require a longer recovery period upon return to normoxia, perhaps at the cost of decreased muscle function from enzyme and contractile apparatus inhibition at low pH. A general strategy amongst animals is that inhibition of function and/or an '*O_2 debt*' (a term used to describe the extra requirement of O_2 following exhaustive exercise required to clear acid and lactate from the muscles) tend to be avoided unless absolutely necessary to avoid the chances of predation if muscle function is impeded (i.e. in diving mammals, Hindell et al., 2000). Overwintering goldfish are also found to maintain muscle function to search out relatively O_2-rich areas (Nilsson, 2001)). These observations suggest that there must be an inhibition of H^+ excretion across the gills in goldfish acclimated to colder temperatures and impaired muscle function is tolerated to achieve systemic pH regulation. Otherwise, there appears to be a contradiction in the priorities of maintaining muscle function in hypoxia and hypercapnia.

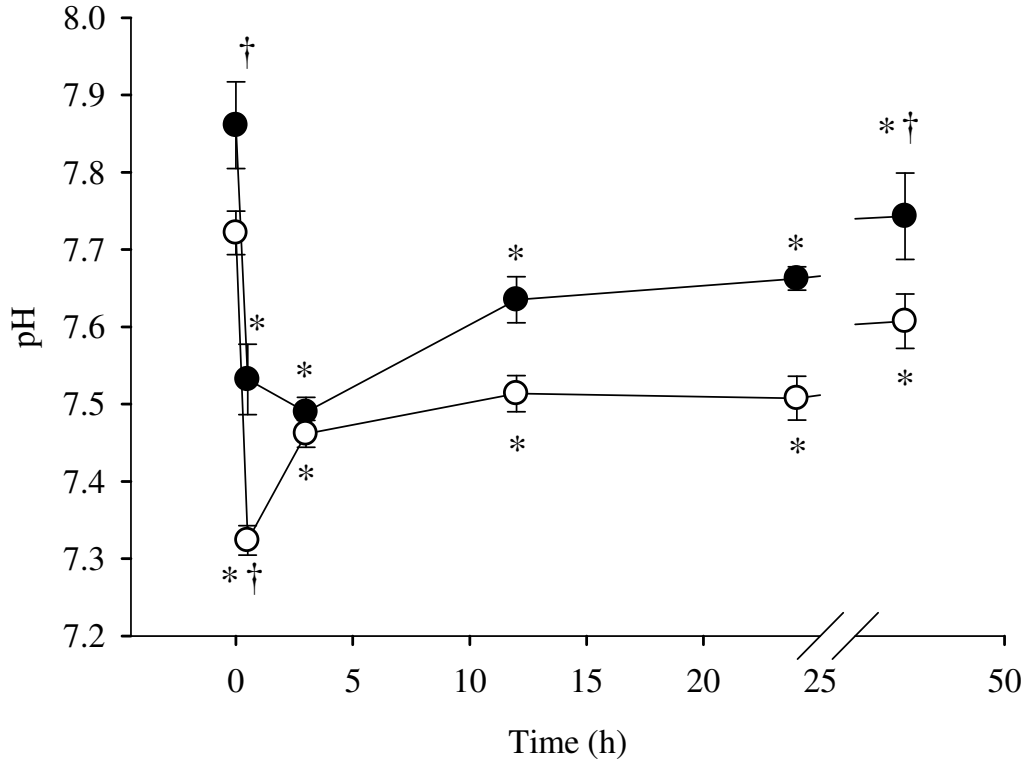
8.0
7.9
7.8
7.7
7.6
7.5
7.4
7.3
7.2
pH
0
5
10
15
20
25
50
Time (h)

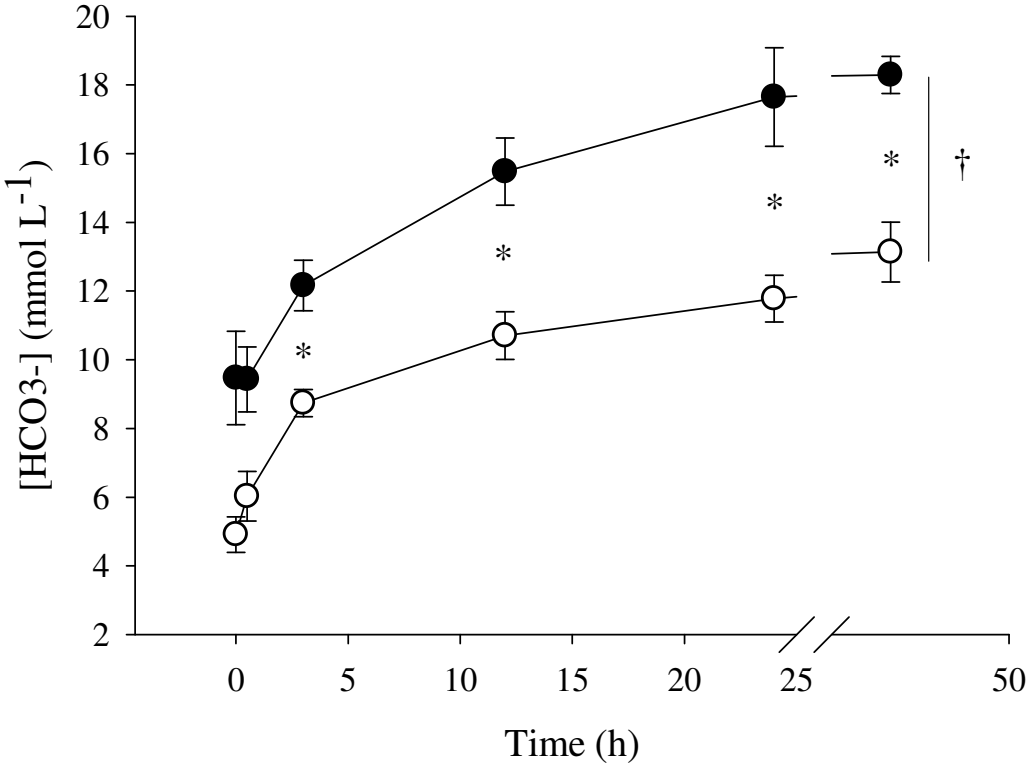
20
18
16
14
12
10
8
6
4
2
[HCO3-] (mmol L-1)
0
5
10
15
20
25
50
Time (h)

Figure 4.1

Whole blood acid-base status of goldfish, *Carassius auratus,* acclimated to 25°C (open circles, n = 7) and 7°C (filled circles, n = 7) and exposed to environmental hypercapnia (P_wCO_2= 10 mmHg). Blood pH (A) and [HCO_3^-] (B) were measured over the 48 h exposureperiod. Data are presented as means ± 1 SEM. * indicates statistical difference from starting initial t = 0 data point within temperature groups, † indicates statistical difference between temperature groups at a given time ($P < 0.005$, 2-way repeated measures ANOVA).

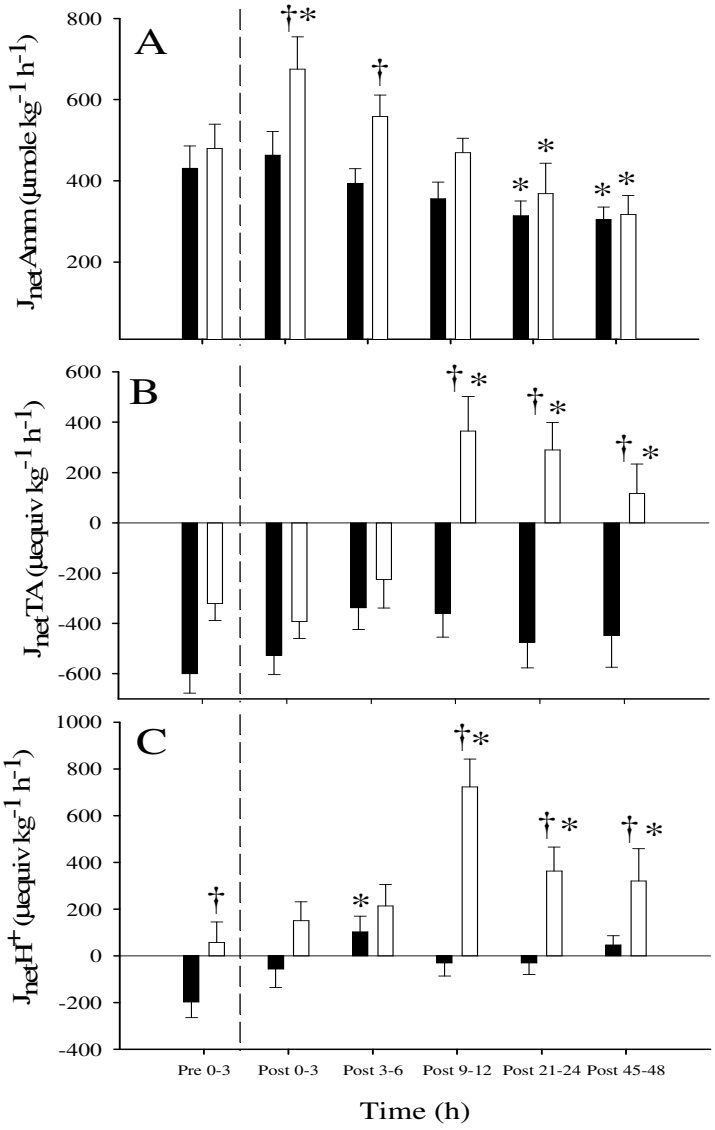
A
B
C
800
600
400
200
-200
-400
1000
-600
$J_{net}Amm$ (µmole kg^{-1} h^{-1})
$J_{net}TA$ (µequiv kg^{-1} h^{-1})
$J_{net}H^+$ (µequiv kg^{-1} h^{-1})
Pre 0-3
Post 0-3
Post 3-6
Post 9-12
Post 21-24
Post 45-48
Time (h)

Figure 4.2

Effect of hypercapnia exposure (P_wCO_2 = 10 mmHg) on net (A) ammonia (J_{net}Amm) (B) titratable alkalinity (J_{net}TA) and (C) proton equivalent ($J_{net}H^+$) fluxes (filled bars represent 25 degree acclimated fish, n = 18, n = 12, n = 12 and n= 18 for (A), (B) and (C), respectively; unfilled bars represent 7 degree acclimated fish, n = 18, n = 12, n= 12 and n= 18 for (A), (B) and (C), respectively. Data are presented as means ± 1 SEM. * denotes significant differences from the pre-hypercapnic flux period within a temperature group, † denotes significant differences between temperature groups ($P < 0.005$, 2-way repeated measures ANOVA).

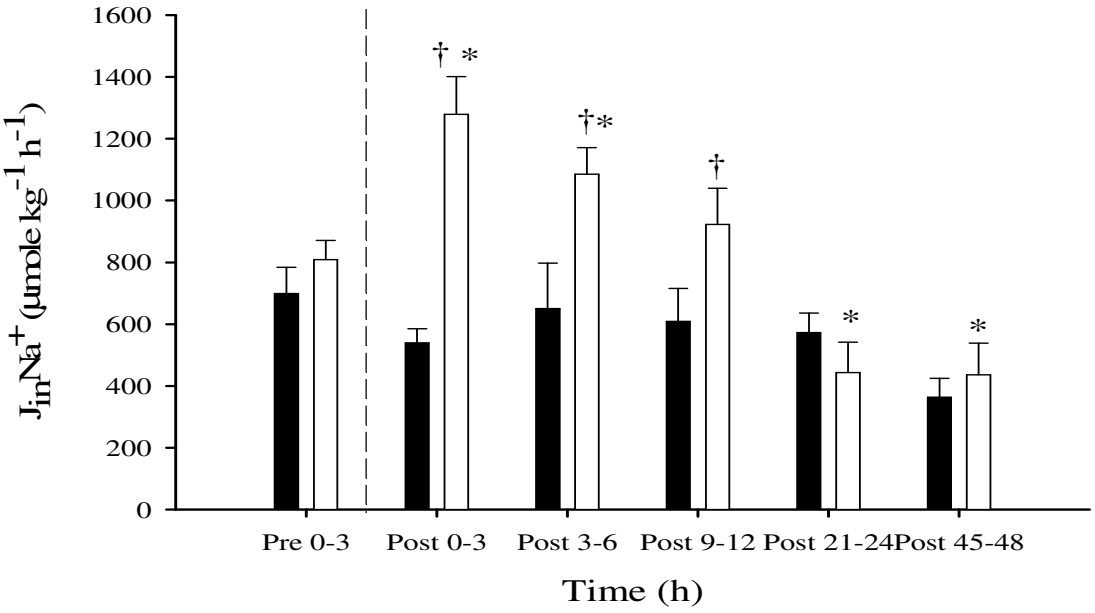
1600
1400
1200
1000
800
600
400
200
0
$J_{in}Na^+$ (µmole kg^{-1} h^{-1})
† *
†*
†
*
*
Pre 0-3
Post 0-3
Post 3-6
Post 9-12
Post 21-24
Post 45-48
Time (h)

Figure 4.3

The effect of environmental hypercapnia exposure on $J_{in}Na^{+}$ in goldfish, *Carassius auratus,* acclimated to 25°C (filled bars) and 7°C (unfilled bars), n = 18 for both. Data are presented as means ± 1 SEM. * indicates significant differences from pre-hypercapnic control period within a temperature group, † indicates significant differences between temperature groups within a time period ($P < 0.005$, 2-way repeated measures ANOVA).

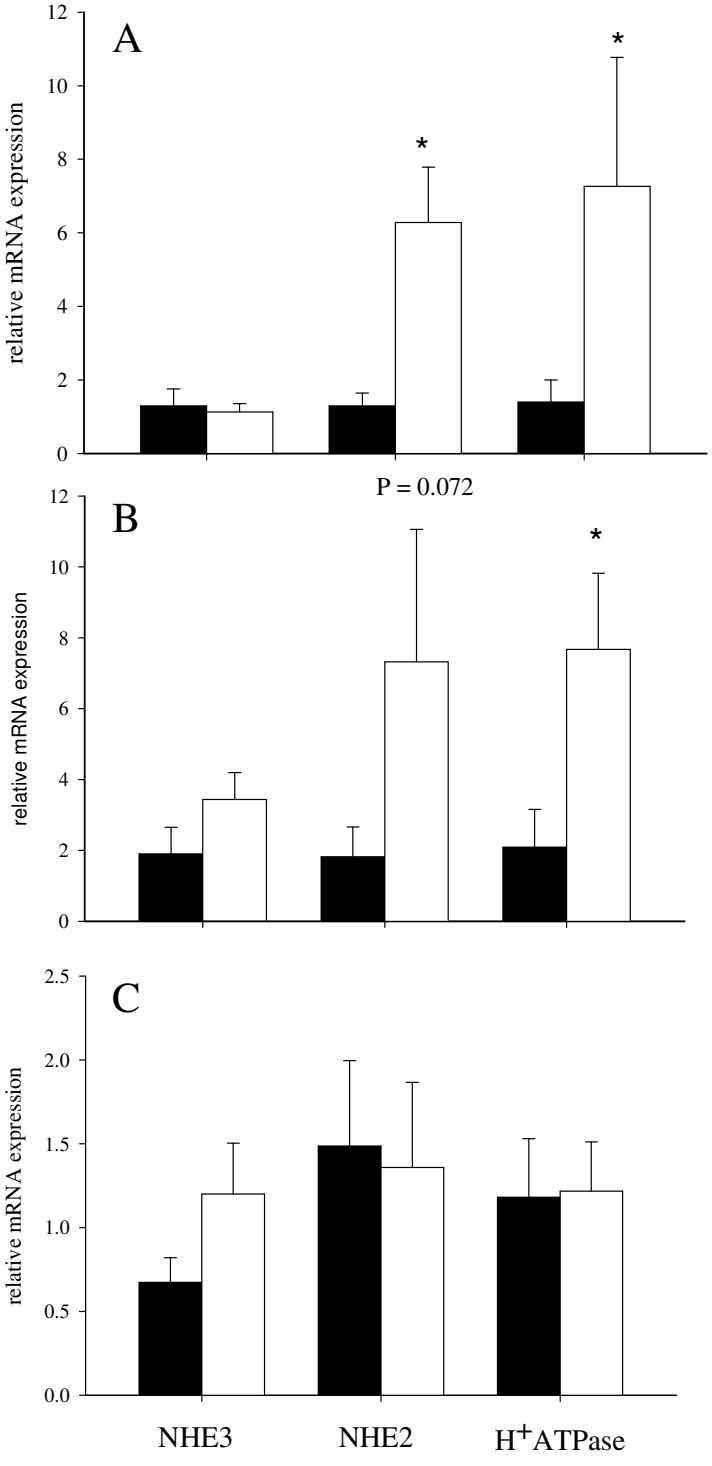
A
B
C
relative mRNA expression
relative mRNA expression
relative mRNA expression
*
*
*
P = 0.072
0
2
4
6
8
10
12
0.0
0.5
1.0
1.5
2.0
2.5
NHE3
NHE2
H+ATPase

Figure 4.4

The effect of CO_2 exposure on relative mRNA expression of NHE3, NHE2 and H^+-ATPase in goldfish, *Caraassius auratus,* acclimated to 7°C (A) and 25°C (B). Filled bars represent normocapnic control fish (n = 6) and unfilled bars represent goldfish exposed to 48 h environmental CO_2 (PCO_2 ~ 10 mmHg) (n = 6). The effect of CO_2 exposure and temperature acclimation is illustrated in (C), where filled bars represent 25°C acclimated fish and unfilled bars represent 7°C acclimated fish exposed to CO_2. * denotes statistical differences between groups ($P < 0.05$, student's t-test). P-values are indicated where ($P < 0.1$, student's t-test). Data are presented as means ± SEM and were calculated by a modified ΔΔCt method where values are expressed relative to 18s and relative to the control (7°C for A and B and 7°C CO_2 exposed for C).

Table 4.1. *Summary of the metabolic exchanges with environment and plasma after 48 h hypercapnia exposure in fish acclimated to 7℃ and 25℃*

Excretion/Uptake (μmol)	**25-degree acclimated**	**7-degree acclimated**	**P-value**
H^+ excreted	104.8 ± 37.2	66.8 ± 23.7	0.39
HCO_3^- accumulated	120.6 ± 43.0	131.1 ± 31.9	0.62

CHAPTER 5.

General Discussion

5.1 Summary of significant findings

The objective of this thesis was to evaluate the effect of gill remodeling on branchial Na^+ transport. Chapter 3 focused on the role of the ILCM as a barrier and to reduce passive Na^+ loss, while Chapter 4 examined the response to respiratory acidosis. I expected to see differences in acid-base regulation between 25°C (w/o an ILCM) and 7°C (w/ an ILCM) acclimated fish *if* the ILCM was found to affect Na^+ flux in Chapter 3.

Chapter 3 revealed a significant effect of temperature acclimation on $J_{out}Na^+$ and $J_{in}Na^+$. Limitations in the experimental design, however, did not permit a conclusive determination of whether $J_{out}Na^+$ was reduced by the ILCM and/or because of an inhibitory effect of temperature. Remodeling following hypoxia exposure did not lead to an increase in $J_{out}Na^+$, which may have resulted from metabolic downregulation and 'channel arrest' associated with limited O_2 availability (see Lutz and Nilsson, 1997). Even following a metabolic recovery in normoxia there was no stimulation of efflux in 7°C fish lacking an ILCM. This result is puzzling considering that Cl^- and PEG efflux (used as an indication of paracellular flux) were markedly stimulated following a return to normoxia in hypoxia-acclimated goldfish (Mitrovic et al., 2009). This observation suggests that metabolic recovery in the fish from the current study was not complete after 12 h normoxia or that Na^+ is regulated independently of branchial surface area or finally that growth of the cell mass had been stimulated to a small extent by 12 h. Although the latter is purely speculative, considering the quick response (remodeling within 12 h normoxia exposure) of the Qinghai carp in the re-growth of its cell mass and the inter-individual variation among ILCM responses in goldfish, it is plausible that ILCM re-growth may have started. The cells responsible for Na^+-uptake, as determined by their

expression of genes pertinent to Na^+ transport (NHE3, NHE2 and H^+-ATPase) were re-distributed from the filamental epithelium to the edge of the ILCM. NHE2 expression was not detected by *in situ* hybridization, but its presence in the gill was confirmed by real-time PCR. Many of the NHE3 expressing cells at the edge of the ILCM appeared to be 'stretched out' to establish contact points with the external environment, the lamellar epithelium or both (Figures 2.10 B and 2.11 B, D), suggesting that they maintain their ion uptake function in the ILCM. That ion-uptake cells are able to maintain their functionality is also supported by constant plasma [Na^+] at all temperatures and regardless of branchial SA, with the exception of hypoxia (Table 3.1).

In chapter 4, the effect of gill remodeling on the capacity for acid-base regulation was examined. The ILCM had no effect on systemic pH regulation during hypercapnia exposure. Blood pH recovered to the same extent and with the same time-course in goldfish acclimated to 7 and 25°C owing to increases in plasma HCO_3^- that were similar in the two groups (Figure 3.1 A and B, respectively). Rather, the ILCM appeared to affect the *mechanism* of acid excretion to the water. In goldfish without an ILCM, Na^+ uptake and NH_3 (NH_4^+) excretion were stimulated immediately and transiently following the onset of the acidosis, while the bulk of acid was excreted from 9-48 h and independently of Na^+ uptake (see Figures 4.2 and 4.3). This description is consistent with what is known about goldfish and carp acid-base regulation (Claiborne and Heisler, 1984; 1986).

In goldfish acclimated to 7°C, on the other hand, the excretion of the entire acid load was unrelated to Na^+ uptake and was likely mediated by Cl^-/HCO_3^- exchange (Figures 4.2 and 4.3). The amount of HCO_3^- accumulated in blood plasma over the 48 h

exposure period was not matched by an equivalent amount of acid excreted to the water in 7°C goldfish, which suggests that H^+ are sequestered in the muscle and released over a longer time scale. This potentially 'altruistic' buffering capacity of the white muscle has been described previously in trout (Wood and LeMoigne, 1991) and in mammals, where it is believed to involve H^+/K^+-exchange across the muscle epithelium (Williams and Epstein, 1989). Another possibility is that H^+ are sequestered into RBCs, whose buffering capacity is qualitatively similar to the white muscle in fishes (Wood and LeMoigne, 1991). In the case of the goldfish this strategy could potentially cause a decrease in Hb oxygen carrying capacity because of the presence of a Root effect Hb (Torracca et al., 1977). That there are mechanistic differences in pH regulation between warm and cold acclimated goldfish is clear. However, further work is needed to confirm the role of the muscle and/or other intracellular compartments (i.e. red blood cell) uniquely in the acid-base regulation of cold-acclimated fish.

5.2 Bridging Na^+ transport and acid-base regulation with gill remodeling in goldfish

The connection between acid-base regulation and ion transport in water-breathing fish is uncontested; acid-base regulation in fish occurs by metabolic acid excretion or base uptake across the branchial epithelium in exchange for Na^+ and Cl^-, respectively (see Perry and Gilmour, 2006 for review). Contributions from the kidney, while more significant in FW compared to SW fish, are still quantitatively insignificant in comparison to gill activity (see section 4.4). Acid equivalents are excreted in exchange for Na^+ (as previously mentioned via NHE or H^+-ATPase/ENaC) while basic equivalents are exchanged for Cl^- (via Cl^-/HCO_3^- anion exchanger). Little is known about the

mechanisms of systemic acid-base regulation in goldfish. Comparison to the carp model (Claiborne and Heisler, 1984) suggests that there is actually little reason to suspect that altered Na^+ transport would affect acid-base regulation. A broadly similar reliance (~75%) on Cl^-/HCO_3^- exchange is assumed to be responsible for the acid-base compensation in the current study (^{36}Cl is no longer commercially available so the transfer of Cl^- could not be measured directly), as only a small portion (~25%) of acid excretion is associated with Na^+ influx in the 25°C fish. The capacity to increase Na^+ influx and the associated acid excretion appears to be the main difference between acid-base regulation in goldfish acclimated to cold and warm temperatures and it is tempting to attribute this change to the presence of the ILCM. However, there is no known rationale to explain why Na^+ uptake or acid-secretion through the ILCM might be different than Cl^- transport. There was no effect of the ILCM on Cl^- transport following thermal acclimation (Mitrovic and Perry, 2009) whereas Na^+ transport may be limited by the ILCM, as indicated by the measured net fluxes. The ILCM had no effect on the time course or extent of pH regulation in this study.

5.3 Ecological significance

If the observed effects of Na^+ efflux are the result of temperature and not because of differences in ILCM, then it begs the question: Why remodel the gills? The purported reasons for adaptively remodeling the gill in goldfish and crucian carp, as stated in Nilsson (2007) are potentially to decrease energy costs associated with osmoregulation, decrease the available surface area for entry of pathogens and toxins and/or protect the gill from hemorrhage by increasing the mass surrounding the lamellae (i.e. providing

structural support). If there are no associated decreases in energy expenditure associated with osmoregulation or any other energetically expensive process, then why grow a mass of cells, which undoubtedly requires the mobilization of resources at a time when it is beneficial to *create* energy stores? It is not likely, in my opinion, that gill remodeling evolved from selection pressures resulting from pathogen exposure. Although goldfish and carp are susceptible to parasitic infection, especially from Ick (*Ichthyophthirius multifiliis*), the parasitic life cycle is slowed down considerably at low temperatures and the largest threat to the organism occurs at higher temperature (Dickerson, 2006). In fact, ick outbreaks in wild populations are more prominent in the early spring after the winter thaw (Dickerson, 2006). Further, why would this adaptation have arisen in these select few species? Unless overwintering, or physiological adaptations related to overwintering confers an extra risk to parasitic infection, it is an unlikely candidate as a selection pressure. Remodeled gills would be structurally more protected, however, the environment in which goldfish live (i.e. slow-moving, pond environment) would not appear to require hardy gills. On the other hand, blood is more viscous at lower temperatures and the ILCM may protect the lamellar blood channels from perfusion damage (Nilsson, 2007), however the need to move blood through the circulatory system is reduced and the reduced flow may alleviate the potential strain of pumping viscous blood through the system. The exact motivation for gill remodeling has not been demonstrated, although, the energy budget hypothesis proposed by Nilsson (2007) is the most likely and ecologically relevant hypothesis, even though an energetic advantage has yet to be experimentally demonstrated.

5.4 Unanswered questions and future directions

Clearly, confounding factors of temperature and environmental oxygen have complicated the assessment of ILCM function. Recently it was shown that gill remodeling is induced through exercise (C Fletcher, K Gilmour, V Tzaneva and SF Perry, unpublished results) and in a relatively quick fashion. This strategy would enable the loss of the cell mass at a constant temperature. Exhaustive exercise would result in a metabolic acidosis and lactate accumulation in the blood and muscles. During recovery, Na^+ and/or Cl^- transport would be stimulated at the gill, possibly confusing assessment of branchial ion flux. Thus, care would need to be taken to *not* exercise fish to exhaustion or to allow sufficient recovery time prior to experimentation (although not long enough for remodeling to take place). Exercise then may provide a useful setting to evaluate the effect of only the ILCM on branchial ion fluxes.

Moreover, if the general proposition is that gill remodeling is driven by the demands of the osmorespiratory compromise, the ion-gas ratio (IGR) can be measured directly in a similar fashion to Gonzalez and McDonald (1992). In this study, they measured MO_2 and $J_{out}Na^+$ simultaneously during exercise and observed an increase in the IGR such that losses of Na^+ were disproportionately increased compared to MO_2 in the rainbow trout. If the ILCM in goldfish reduces ion efflux, ion efflux should be decreased to a much greater extent than MO_2, considering there is no impedance of O_2 transport. Of course there are many other factors affecting the permeability of the gill including the depth and number of TJ proteins (Cerejido and Anderson, 2001; Chasiotis et al., 2009) and circulating catecholamines (Vermette and Perry, 1987).

An experiment must also be completed to confirm the role of intracellular compartments in acid-base regulation in goldfish with an ILCM. The time-course of the hypercapnia exposure should be increased if a model of delayed excretion of acid equivalents to the water is occurring in cold-acclimated fish. Measurements of the intracellular pH in goldfish white muscle in cold-acclimated fish exposed to hypercapnia compared to controls should indicate if an acid load is retained in the muscle. Furthermore, it would be interesting to measure the extent of gill remodeling following prolonged hyperpcania, if any, in cold-acclimated goldfish. Considering that an acidosis lowers the O_2 carrying capacity of the blood in fish with a Root effect Hb, if the stimulus to remodel is in fact O_2 demand, it follows that a decrease in systemic pH, if prolonged or sufficiently severe, ought to initiate gill remodeling.

5.5 Conclusions

The results of this thesis suggested an effect of the ILCM on branchial Na^+ transport and also revealed limitations in the experimental design that could not be controlled for (i.e. temperature), demonstrated a re-distribution of putative Na^+-uptake cells to the edge of the cell mass and revealed differences in acid-base regulation strategies imposed by the ILCM.

REFERENCES

Avella M and Bornancin M (1989). A new analysis of ammonia and sodium transport through the gills of the freshwater rainbow trout (*Salmo gairdneri)*. *J. Exp. Biol.* **142,** 155-175.

Barron MG, Tarr BD, Hayton WL (1987). Temperature-dependence of cardiac output and regional blood flow in rainbow trout, *Salmo gairdneri*. *J. Fish. Biol.* **31,** 735-744.

Bindon SD, Gilmour KM, Fenwick JC, Perry SF (1994). The effects of branchial chloride cell-proliferation on respiratory-function in the rainbow-trout *Oncorhynchus mykiss*. *J. Exp. Biol.* **197,** 47-63.

Boeuf G and Payan P (2001). How should salinity influence fish growth? *Comp Biochem Physiol Part C* **130,** 411-423.

Boisen AM, Amstrup J, Novak I, Grosell M (2003). Sodium and Chloride transport in soft water and hard water acclimated zebrafish (*Danio rerio)*. *Biochim. Biophys. Acta.* **1618,** 207-218.

Booth JH (1978). Distribution of blood flow in the gills of fish – application of a new technique to rainbow-trout (*Salmo-gairdneri)*. *J Exp Biol.* **73,** 119-129.

Braun MH, Steele SL, Ekker M, Perry SF (2009). Nitrogen excretion in developing zebrafish (*Danio rerio*): a role for Rh proteins and urea transporters. *Am. J. Physiol. Renal Physiol.* **296,** F994-F1005.

Burgess DW, Marshall WS, Wood CM (1998). Ionic transport by the opercular epithelia of freshwater acclimated tilapia (*Oreochromis niloticus*) and killifish (*Fundulus heteroclitus*). *Comp. Biochem. Physiol. Mole. Integr. Physiol.* **121,** 155-164.

Burggren WW (1982). Air gulping improves blood oxygen transport during aquatic hypoxia in the goldfish *Carassius auratus*. *Physiol. Zool.* **55,** 327-334.

Cameron JN (1980). Body fluid pools, kidney function and acid-base regulation in the freshwater catfish, *Ictalurus punctatus*. *J. Exp. Biol.* **86,** 171-185.

Catlett RH and Millich DR (1976). Intracellular and extracellular osmoregulation of temperature acclimated goldfish *Carassius auratus* L. *Comp. Biochem. Physiol.* **55,** 261-269.

Cereijido M and Anderson JM (2001). Introduction: evolution of ideas on tight junction. In *Tight Junctions* (ed. M. Cereijido and J.M. Anderson), p. 1-18. Boca Raton: CRC Press.

Chasiotis H and Kelly SP (2008). Occludin immunolocalization and protein expression in goldfish. *J Exp. Biol.* **211,** 1524-1534.

Chasiotis H, Effendi JC, Kelly SP (2009). Occludin expression in goldfish held in ion poor water. *J Comp Physiol B*. **179,** 145-154.

Chasiotis H, Wood CM, Kelly SP (2010). Cortisol reduces paracellular permeability and increases occluding abundance in cultured trout gill epithelia. *Mol Cell Endocrinol* **323,** 232-238.

Claiborne JB and Heisler N (1984). Acid-base regulation and ion transfers in the carp (*Cyrpinus carpio*) during and after exposure to environmental hypercapnia. *J Exp Biol*. **108,** 25-43.

Claiborne JB and Heisler N (1986). Acid-base regulation and ion transfers in the carp (*Cyprinus carpio*): pH compensation during graded long- and short-term environmental hypercapnia, and the effect of bicarbonate infusion. *J Exp Biol* **126,** 41-61.

Colegio OR, Itallie CV, McCrea HJ, Rahner C, Anderson JM (2002). Claudins create charge-selective channels in the paracellular pathway between epithelial cells. *Am J Physiol. Cell Physiol.* **283,** C142-C147.

De Jager S and Dekkers WJ (1975). Relation between gill structure and activity in fish. *Neth. J. Zool.* **25,** 276-308.

De Jager S, Smit-Onel ME, Videler JJ, Van-Gills BJM and Uffink EM (1977). The respiratory area of the gills of some teleost fishes in relation to their mode of life. *Bijdr. Dierk.* **46,** 199-205

Diaz RJJ (2001). Overview of hypoxia around the world. *Journ. Env. Qual.* **30,** 275-281.

Dickerson HW (2006). Ichthyophthirius multifiliis In: *Fish Diseases and Disorders. Vol 1: Protozoan and Metazoan Infections* (ed. Woo, PTK). CABI, Oxfordshire, UK, p 118-119.

Edwards SL, Weakley JC, Diamanduros AW, Claiborne JB (2010). Molecular identification of Na^+-H^+ exchanger isoform (NHE2) in the gills of the euryhaline teleost *Fundulus heteroclitus. J Fish Biol.* **76,** 415-426.

Esaki M, Hoshijima K, Kobayashi S, Fukuda H, Kawakami K, Hirose S (2006). Visualization in zebrafish larvae of Na^+ uptake in mitochondria-rich cells whose differentiaion is dependent on *foxi3a*. *Am. J. Physiol. Regul. Integr. Comp. Physiol.* **292,** R470-R480.

Evans DH (2008). Teleost fish osmoregulation: what have we learned since August Krogh, Homer Smith and Ancel Keys. *Am J Physiol. Regul. Integr. Comp. Physiol.* **295,** R704-R713.

Evans RE, Brown SB, Hara TJ (1988). The effects of aluminum and acid on the gill morphology in rainbow trout, *Salmo gairneri*. *Env. Biol. Fishes* **22** (4), 299-311.

Farrell AP (1980). Vascular pathways in the gill of ling cod, *Ophiodon elongates*. *Can. J. Zool.* **58,** 796-806.

Fenwick JC, Wendelaar Bonga SE, Flik G (1999). In vivo bafilomycin-sensitive Na^+ uptake in young freshwater fish. *J Exp. Biol.* **202,** 3659-3666.

Galvez F, Reid SD, Hawkings G, Goss GG (2001). Isolation and characterization of mitochondria-rich cell types from the gill of freshwater rainbow trout. *Am J Phyiol Reg Comp Physiol.* **282,** R658-R668.

Gilmour KM and Perry SF (2009). Carbonic anhydrase and acid-base regulation in fish. *J Exp Biol.* **212,** 1647-1661.

Gonzalez RJ and McDonald DG (1992). The relationship between oxygen consumption and ion loss in a freshwater fish. *J. Exp. Biol.* **163,** 317-322.

Goss GG, Adamia S, Galvez F (2001). Peanut lectin binds to a subpopulation of mitochondria rich cells in the rainbow trout gill epithelium. *Am. J. Physiol. Regulatory Integrative Comp. Physiol.* **281,** R1718-1725.

Goss GG, Laurent P, Perry SF (1992). Gill morphology and acid-base regulation in during hypercapnic acidosis in the brown bullhead, *Ictalurus nebulosus. Cell Tissue Res.* **268,** 539-552.

Goss GG, Perrsy SF, Wood CM, Laurent P (1992). Mechanisms of ion and acid-base regulation at the gills of freshwater fish. *J Exp Zool.* **263,** 143-159.

Goss GG and Perry SF (1993a). Physiological and Morphological regulation of acid-base status during hypercapnia in rainbow trout (*Oncorhynchus mykiss). Can. J. Zool.* **71**, 1673-1680.

Goss GG, Laurent P, Perry SF (1993b). Evidence for a morphological component in acid-base regulation during environmental hypercapnia in the brown bullhead, (*Ictalurus nebulosus). Cell Tissue Res.* **268,** 539-552.

Greco AM, Gilmour KM, Fenwick JC, Perry SF (1995). The effects of softwater acclimation on respiratory gas transfer in the rainbow trout *Oncorhynchus mykiss*. *J. Exp. Biol.* **198,** 2557-2567.

Greco AM, Fenwick JC, Perry SF (1996). The effects of soft-water acclimation on gill structure in the rainbow trout *Onchorhynchus mykiss*. *Cell Tissue Res.* **285,** 75-82.

Hazel JR (1984). Effects of temperature on the structure and metabolism of cell membranes in fish. *Am. J. Physiol.* **246,** R460-R470.

Heisler N (1978). Bicarbonate exchange between body compartments after changes of temperature in the large spotted dogfish (*Scyliorhinus stellaris*). *Respir. Physiol.* **33,** 145-160.

Heisler N and Neumann P (1980). The role of physico-chemical buffering and of bicarbonate transfer processes in intracellular pH regulation in response to changes of temperature in the larger spotted dogfish (*Scyliorhinus stellaris*). *J. Exp. Biol.* **85,** 99-110.

Heisler N (1984). Acid-base regulation in fishes. In: *Fish Physiology,* vol X. (ed. W.S. Hoar and D.J. Randall), pp 315-401. New York: Academic Press.

Hindell MA, Lea M-A, Morrice MG, MacMahon CR (2000). Metabolic limits on dive duration and swimming speed in the southern elephant seal *Mirounga leonine. Physiol. Biochem. Zool.* **73,** 790-798.

Hiroi J, McCormick SD, Ohtani-Kaneko R, Kaneko T (2005). Functional classification of mitochondrion-rich cells in euyhaline Mozambique tilapia (*Oreochromis mossambicus*) embryos, by means of triple immunofluorescence staining for Na^+/K^+-ATPase, $Na^+/K^+/2Cl^-$ cotransporter and CFTR anion channel. *J Exp Biol.* **208,** 2023-2036.

Hochachka PW (1986). Defense strategies against hypoxia and hypothermia. *Science.* **231,** 234-241.

Houston AH and Madden JA (1968). Environmental temperature and plasma electrolyte regulation in the carp, *Cyprinus carpio*. *Nature* **217,** 969-970.

Houston AH and Mearow KM (1981). Branchial and renal (Na^+/K^+) ATPase and carbonic anhydrase activities in a eurythermal freshwater teleost, *Carassius auratus* L. *Comp. Biochem. Physiol.* **71,** 175-180.

Hughes GM (1966). The dimension of fish gills in relation to their function. *J. exp. Biol.* **45**, 177-95.

Hughes GM and Morgan M (1973). The structure of fish gills in relation to their respiratory function. *Biol Rev.* **48,** 419-475.

Hwang P-P (2009). Ion uptake and acid secretion in zebrafish (*Danio rerio)*. *J. Exp. Biol.* **212,** 1745-1752.

Hwang P-P and Lee T-H (2007). New insights into fish ion regulation and mitochondrion-rich cells. *Comp. Biochem. Physiol. A Mol. Integr. Physiol.* **148,** 479-497.

Hwang P-P and Perry SF (2010). Ionic and acid-base regulation. In: *Fish Physiology.* Vol. 29. (Perry SF, Ekker M, Farrell AP, Brauner CJ eds.) pp. 311-344. Academic Press, London, UK.

Hyde DA and Perry SF (1989). Differential approaches to blood acid-base regulation during exposure to prolonged hypercapnia in two freshwater teleosts: The rainbow trout (*Salmo gairdneri*) and the American eel (*Anguilla rostrata*). *Physiol Zool* **62,** 1164-1186.

Isaia J (1982). Effects of environmental salinity on branchial permeability of rainbow trout, *Salmo gairdneri. J Phyiol.* **326,** 297-307.

Ivanis G, Esbaugh AJ, Perry SF (2008). Branchial expression and localization of SLC9A2 and SLC9A3 sodium/hydrogen exchangers and their possible role in acid-base regulation in freshwater rainbow trout (*Onchorhynchus mykiss*). **211,** 2467-2477.

Iwama GK and Heisler N (1991). Effect of environmental water salinity on acid-base regulation during environmental hypercapnia in the rainbow trout (*Oncorhynchus mykiss*). *J. Exp. Biol.* **158,** 1-18.

Kerstetter TH, Kirschner LB, Rafuse DD (1970). On the mechanisms of sodium ion transport by the irrigated gills of rainbow trout (*Salmo gairdneri). J. Gen. Physiol.* **56,** 342-359.

Kikuchi S (1977). Mitochondria-rich (chloride) cells in the gill epithelia from four species of stenohaline fresh water teleosts. *Cell Tissue Res.* **180,** 87-98.

King PA and Goldstein L (1983). Renal ammonia production in goldfish, *Carassius auratus*. *Am. J. Physiol. Integr. Comp. Physiol.* **245,** 590-599.

Krogh A (1938). The active absorption of ions in some freshwater animals. *Z. Vergl. Physiol.* **25,** 335-350.

Lahlou B, Henderson IW, Sawyer WH (1969). Sodium exchanges in goldfish (*Carassius auratus L.*) adapted to a hypertonic saline solution. *Comp. Biochem. Physiol.* **28,** 1427-1433.

Laurent P (1984). Gill internal morphology. In: *Fish Physiology* (ed. W.S. Hoar) Vol. 10 pp.73-184.

Laurent P, Goss GG, Perry SF (1994). Proton pumps in fish gill pavement cells. *Arch. Int. Physiol. Biochim. Biophys.* **102,** 77-79.

Laurent P and Perry SF (1990). Effects of cortisol on gill chloride cell morphology and ionic uptake in the freshwater trout, *Salmo gairdneri*. *Cell Tissue Res.* **259,** 429-442.

Lee TH, Hwang PP, Lin HC, Huang FL (1996). Mitochondria-rich cells in the branchial epithelium of the teleost, *Oreochromis mossambicus*, acclimated to various hypotonic environments. *Fish Physiol Biochem.* **15,** 513-523.

Lee TH, Hwang PP, Feng SH (1996b). Morphological studies of gill and mitochondria-rich cells in the stenohaline cyprinid teleosts, *Cyprinus carpio* and *Carassius auratus*, adapted to various hypotonic environments. *Zoological Studies*. **35,** 272-278.

Lee TH, Hwang PP, Shieh YE, Lin CH (2000). The relationship between 'deep-hole' mitochondria-rich cells and salinity adaptation in the euryhaline teleost, *Oreochromis mossambicus. Fish Physiol. Biochem.* **23,** 133-140.

LeHir M, Kaissling B, Koeppen BM, Wade JB (1982). Binding of peanut lectin to specific epithelial cell types in kidney. *Am. J. Physiol. Cell Physiol.* **242,** C117-C120.

Lin H, Pfeiffer DC, Vogl AW, Pan J, Randall DJ (1994). Immunolocalization of H^+-ATPase in the gill epithelia of rainbow trout. *J. Exp. Biol.* **195,** 169-183.

Lin H and Randall DJ (1993). H^+-ATPase activity in crude homogenates of fish gill tissue-inhibitor sensitivity and environmental and hormonal regulation. *J. Exp. Biol.* **180,** 163-174.

Lutz PL and Nilsson GE (1997). Contrasting strategies for anoxic brain survival-glycolysis up or down. *J. Exp. Biol.* **200,** 411-419.

Maetz J (1956). Les échanges de sodium chez le poisson *Carassius auratus* L. Action d'un inhibiteur de l'anhydrase carbonique. *J. Physiol (Paris*) **48**, 1085–1099.

Maetz J and Garcia-Romeu F (1964). The mechanisms of sodium and chloride uptake by the gills of a fresh water fish, *Carassius auratus*. II. Evidence for NH_4^+/Na^+ and $HCO3^-/Cl^-$ exchanges. *J. Gen. Physiol.* **47,** 1209-1227.

Maetz J (1972). Branchial sodium exchange and ammonia excretion in the goldfish *Carassius auratus*. Effect of ammonia loading and temperature changes. *J Exp. Biol.* **56,**

Marshall WS (2002). Na+, Cl-, Ca2+ and Zn2+ transport by fish gills: a retrospective review and prospective synthesis. *J. Exp. Zool.* **293,** 264-283.

Matey V, Richards JG, Wang Y, Wood CM, Rogers J, Davies R, Murray BW, Chen X-Q, Du J, Brauner CJ (2008). The effect of hypoxia on gill morphology and ionoregulatory status in the Lake Qinghai scaleless carp, *Gymnocypris przewalskii*. *J. Exp. Biol.* **211,** 1063-1074.

McDonald DG and Rogano MS. (1986). Ion regulation by the rainbow trout, *Salmo gairdneri*, in ion poor water. *Physiol. Zool.* **59,** 318-331.

McDonald DG and Wood CM (1981). Branchial and renal acid and ion fluxes in the rainbow trout, *Salmo gairdneri*, at low environmental pH. *J. Exp. Biol.* **93,** 101-118.

Meuwis AL and Heuts MJ (1957). Temperature dependence of breathing rate in carp. *Biol. Bull.* **112,** 97-107.

Mitrovic D, Dymowska A, Nilsson GE, Perry SF (2009). Physiological consequences of gill remodeling in goldfish (*Carassius auratus*) during exposure to long-term hypoxia. *Am J Phyiol Regul Integr Comp Physiol* **297,** R224-R234.

Mitrovic D and Perry SF (2009). The effects of thermally induced gill remodeling on ionocyte distribution and branchial chloride fluxes in goldfish (*Carassius auratus). J. Exp. Biol.* **212,** 843-852.

Murphy PG and Houston AH (1973). Environmental temperature and the body fluid system of the fresh-water teleost – Plasma electrolyte levels and branchial microsomal (Na^+-K^+) ATPase activity in the thermally acclimated goldfish (*Carassius auratus*). *Comp. Biochem. Physiol.* **47,** 563-570.

Nakada T, Hoshijima K, Esaki M, Nagayoshi S, Kawakami K, Hirose S (2007a). Localization of ammonia transporter Rhcg1 in mitochondrion-rich cells of yolk sac, gill and kidney of zebrafish and its ionic strength-dependent expression. *Am. J. Physiol. Regul. Integr. Comp. Physiol.* **293,** R1743-1753.

Nakada T, Westhoff CM, Kato A, Hirose S (2007b). Ammonia secretion from fish gill depends on a set of Rh glycoproteins. *FASEB J.* **21,** 1067-1074.

Nawata CM, Hung CC, Tsui TK, Wilson JM, Wright PA, Wood CM (2007). Ammonia excretion in rainbow trout (*Oncorhynchus mykiss*): evidence for Rh glycoprotein and H^+-ATPase involvement. *Physiol. Genomics*. **31,** 463-474.

Nilsson S and Sundin L (1986). Gill blood flow control. *Comp. Biomchem. Physiol. A Mol. Integr. Physiol.* **119,** 137-147.

Nilsson GE (2001). Surviving with the brain turned on. *News Physiol Sci* **16,** 217-221.

Nilsson GE (2007). Gill remodeling in fish – a new fashion or ancient secret? *J Exp Biol.* **210,** 2403-2409.

Ong KJ, Stevens ED, Wright PA (2007). Gill morphology of the mangrove killifish (*Kryptolebias marmoratus*) is plastic and changes in response to terrestrial air exposure. *J. Exp. Biol.* **210,** 1109-1115.

Parks SK, Tresguerres M, Goss GG (2008). Theoretical considerations underlying Na^+ uptake mechanisms in freshwater fishes. *Comp. Biochem. Physiol. Part C.* **148,** 411-418.

Payan P (1978). A study of the Na^+/NH_4^+ exchange across the gill of the perfused head of the trout (*Salmo gairdneri*). *J. Comp. Physiol.* **124,** 181-188.

Perry SF (1997). The Chloride Cell: Structure and function in the gills of freshwater fishes. *Ann. Rev. Physiol.* **59,** 325-347.

Perry SF (1998). Relationships between branchial chloride cells and gas transfer in freshwater fish. *Comp Biochem Physiol A*. **119,** 9-16.

Perry SF, Braun MH, Genz J, Vulsevic B, Taylor J, Grosell M, Gilmour KM (2010). Acid-base regulation in the plainfin midshipman (*Porichthys notatus*): an aglomerular marine teleost. *J. Comp. Physiol. B.* In Press.

Perry SF, Furimsky M, Bayaa M, Georgalis T, Nickerson JG, Moon TW (2003). Integrated involvement of Na^+/HCO_3^- cotransporters and V-type H^+-ATPase in branchial and renal acid-base regulation in freshwater fishes. *Biochem. Biophys. Acta.* **1618,** 175-184.

Perry SF, Haswell MS, Randall DJ, Farrell AP (1981). Branchial ion uptake and acid-base regulation in the rainbow trout, *Salmo gairdneri*. *J. Exp. Biol.* **92,** 289-303.

Perry SF and Gilmour KM (2006). Acid-base balance and CO_2 excretion in fish: unanswered questions and emerging models. *Respir. Physiol. Neurobiol.* **154,** 199-215.

Perry SF, Goss GG, Laurent P (1992). The interrelationships between gill chloride cell morphology and ionic uptake in four freshwater teleosts. *Can. J. Zool.* **70**, 1737-1742.

Perry SF, Haswell MS, Randall DJ, Farrell AP (1981). Branchial ionic uptake and acid-base regulation in the rainbow trout, *Salmo gairdneri*. *J. Exp. Biol.* **92,** 289-303.

Perry SF and Laurent P (1989). Adaptational responses of rainbow trout to lowered external NaCl concentration: contribution of the branchial chloride cell. *J. Exp. Biol.* **147,** 147-168.

Perry SF, Malone S, Ewing D (1987). Hypercapnic acidosis in the rainbow trout (*Salmo gairdneri*). I. Branchial ionic fluxes and blood acid-base status. *Can J Zool.* **65,** 888-895.

Perry SF, Schwaiger T, Kumai Y, Tzaneva T, Braun MH (2010). The consequences of reversible gill remodeling on ammonia excretion in goldfish (*Carassius auratus*). *J Exp Biol.* **213,** 3656-2665.

Pfaffl MW (2001). A new mathematical model for relative quantification in real-time PCR. *Nucleic Acids Res.* **29** (9), e45.

Preest MR, Gonzalez RJ, Wilson RW (2005). A pharmacological examination of Na^+ and Cl^- transport in two species of freshwater fish. *Physiol. Biochem. Zool.* **78,** 259-272.

Prosser CL, Mackay W, Kato K (1970). Osmotic and ionic concentrations in some Alaskan fish and goldfish from different temperatures. *Phyiol. Zool.* **43,** 81-89.

Randall DJ, Baumgarten D and Malyusz M (1972). The relationship between gas and ion transfer across the gills of fishes. *Comp. Biochem. Physiol.* **41,** 629-637.

Randall DJ and Wright PA (1987). Ammonia distribution and excretion in fish. *Fish Physiol. Biochem.* **3,** 107-120.

Reeves RB (1977). The interaction of body temperature and acid-base balance in ectothermic vertebrates. *Ann. Rev. Physiol.* **39,** 559-586.

Sardet C, Pisam M, Maetz J (1979). The surface epithelium of Teleostean fish gills: cellular and junctional adaptations of chloride cell in relation to salt adaptation. *J. Cell. Biol.* **80,** 96-117.

Shoubridge EA and Hochachka PW (1980). Ethanol: Novel end product of vertebrate anaerobic metabolism. *Science*. **209,** 308-309.

Sheratt BM, Jones IC, Bellamy B (1964). Water and electrolyte composition of the body and renal function of the eel (*Anguilla anguilla L.*). *Comp. Biochem. Physiol.* **11,** 9-18.

Sloman KA, Gilmour KM, Metcalfe NB, Taylor AC (2000). Does socially induced stress in rainbow trout cause chloride cell proliferation? *J Fish Biol.* **56,** 725-738.

Smith A, Zhang J, Guay D, Quint E, Johnson A, Akimenko MA (2008). Gene expression analysis on sections of zebrafish regenerating fins reveals limitations in the whole-mount *in situ* hybridization method. *Dev. Dyn.* **237** (2), 417-425.

Sollid J, De Angelis P, Gundersen K, Nilsson GE (2003). Hypoxia induces adapative and reversible gross morphological changes in crucian carp gills. *J Exp Biol* **206,** 3667-3673.

Sollid J and Nilsson GE (2006). Plasticity of respiratory structures- Adaptive remodeling of fish gills induced by ambient oxygen and temperature. *Respiratory Physiol Neurobiol*. **154,** 241-251.

Sollid J, Rissanen E, Tranberg HK, Thorstensen T, Vuori KAM, Nikinmaa M, Nilsson GE (2006). HIF-1α and iNOS levels in crucian carp gills during hypoxia-induced transformation. *J Comp Physiol B*. **176,** 359-369.

Sollid J, Weber RE, Nilsson GE. (2005). Temperature alters the respiratory surface area of crucian carp (*Carassius carassius)* and goldfish (*Carassius auratus*). *J. Exp. Biol.* **208,** 1109-1116.

Sullivan GV, Fryer JN, Perry SF (1995). Immunolocalization of proton pumps (H^+-ATPase) in pavement cells in rainbow trout gill. *J. Exp. Biol.* **198,** 2619-2629.

Torracca AMV, Raschetti R, Salvioli R, Ricciardi G, Winterhalter KH (1977). Modulation of the root effect in goldfish by ATP and GTP. *Biochim. Biophys. Acta.* **28,** 367-373.

Towle DW, Rushton ME, Heidysch D, Magnani JJ, Rose MJ, Amstutz A, Jordan MK, Shearer DW, Wu WS (1997). Sodium/proton antiporter in the euryhaline crab *Carcinus meanus*: molecular cloning, expression and tissue distribution. *J. Exp. Biol.* **200,** 1003-1014.

Tresguerres M, Katoh F, Fenton H, Jasinska E, Goss GG (2005). Regulation of branchial V-H^+-ATPase, Na^+/K^+-ATPase and NHE2 in response to acid and base infusions in the Pacific spiny dogfish (*Squalus acanthias*). *J. Exp. Biol.* **208,** 345-354.

Umminger BL (1969). Patterns of osmoregulation in freshwater fishes at temperatures near freezing. *Physiol Zool.* **44,** 20-27.

Verdouw H, van Echted CJA, Dekkers EMJ (1978). Ammonia determination based on indophenol formation with sodium salicylate. *Water Res.* **12,** 399-402.

Vermette MG and Perry SF (1987). The effects of prolonged epinephrine infusion on the physiology of the rainbow trout, *Salmo gairneri*. II. Branchial solute fluxes. *J. Exp. Biol.* **128,** 255-267.

Williams ME and Epstein FH (1989). Internal exchanges of potassium. In: The Regulaton of Potassium Balance, edited by DW Seldin and G Giebisch, New York, Raven Press, p 3-29.

Wilson JM and Laurent P (2002). Fish gill morphology: Inside out. *J Exp Zool.* **293,** 192-213.

Wood CM, Iftikar FI, Scott GR, De Boeck G, Sloman KA, Matey V, Domingos FX, Duarte RM, Almeida-Val VMF, Val AL (2009). Regulation of gill transcellular permeability and renal function during acute hypoxia in the Amazonian oscar (*Astronotus ocellatus*): new angles to the osmorespiratory compromise. *J. Exp. Biol.* **212,** 1949-1964.

Wood CM, Kajimura M, Sloman KA, Scott GR, Walsh PJ, Amerida-Val VMF, Val AL. (2007). Rapid regulation of Na^+ fluxes and ammonia excretion in response to

acute environmental hypoxia in the Amazonian oscar, *Astronotus ocellatus*. *Am. J. Physiol.* **292,** R2048-R2058.

Wood CM and LeMoigne J (1991). Intracellular acid-base responses to environmental hyperoxia and normoxic recovery in rainbow trout. *Resp. Physiol.* **86,** 91-113.

Wright PA, Randall DJ and Wood CM (1988). The distribution of ammonia and H+ between tissue compartments in lemon sole (*Parophrys vetulus*) at rest, during hyperapnia and following exercise. *J. Exp. Biol.* **136,** 149-175.

Wright PA and Wood CM (2009). A new paradigm for ammonia excretion in aquatic animals: role of Rhesus (Rh) glycoproteins. *J Exp Biol.* **212,** 2303-2312.

Yan J-J, Chou M-Y, Kaneko T, Hwang P-P (2007). Gene expression of Na^+/H^+ exchanger in zebrafish H+-ATPase-rich cells during acclimation to low Na^+ and acidic environments. *Am. J. Physiol. Cell Physiol.* **293,** C1814-C1823.

Zadunaisky JA (1984). The chloride cell: the active transport of chloride and the paracellular pathways. In: *Fish Physiology* Vol. 10B. (WS Hoar and DJ Randall, eds.) pp. 129-176. Academic Press, New York.